2011

Development and validation of biomechanical models to quantify horse back forces at the walk in three horse breeds

Laxmi Raghunandana Kaidapuram
Louisiana State University and Agricultural and Mechanical College

DEVELOPMENT AND VALIDATION OF BIOMECHANICAL MODELS TO QUANTIFY HORSE BACK FORCES AT THE WALK IN THREE HORSE BREEDS

A Thesis
Submitted to the Graduate Faculty of the
Louisiana State University and
Agricultural and Mechanical College
in partial fulfillment of the
requirements for the degree of
Master of Science in Electrical Engineering

in

The Department of Electrical and Computer Engineering

by
Laxmi Raghunandana Kaidapuram,
B.Tech in Electronics and Communication Engineering,
Jawaharlal Nehru Technological University, Hyderabad, 2007
December 2011

Acknowledgements

This thesis would not have been possible without the guidance and the help of several individuals who in one way or another contributed and extended their valuable assistance in the preparation and completion of this study.

I am heartily grateful to my advisors, Dr. Martin Feldman and Dr. Mandi J. Lopez (Department of Veterinary Clinical Sciences) whose exemplary support and guidance I will never forget. Dr. Lopez introduced the thesis topic and helped me in understanding the horse anatomical model to use in my work. She taught me how to approach a problem and inspired me how to be patient in dark times when progress is slow. Dr. Feldman taught me how to analyze the engineering concepts optimally. His technical advice and suggestions improved my problem solving abilities. I attribute the level of my Masters degree to their encouragement and effort and without them this thesis, too, would not have been completed or written.

I would like to thank my committee member, Dr. Vaidyanathan for his kind support in thesis and coursework. I also deeply appreciate Dr. Lu Peng, Dr. Alex Skavanzos and Dr. Xin Li for offering me knowledgeable courses.

Furthermore, I thank Dr. Frank Andrews (Equine Health Studies Program) for supporting me financially from my first day in LSU, making me concentrate on my research. I am grateful to Michael Keowen and Dr. Michelle Woodward for allotting their time for data collection.

I thank my fellow labmates in the Laboratory of Equine and Comparative Orthopedic Research: Lin Xie, Dr. Masudul Haque, Nan Zhang, Prakash Babu Bommala, Vanessa Marigo and José Aquiles Parodi Amaya for the stimulating discussions, for the sleepless nights we were working together before deadlines, for collaborative work during data collection and for all the fun we have had in the lab.

Last but not least, my deepest gratitude to my parents: Manjula and Narsimha Reddy, my aunt and uncle: Meena and Kondal Reddy, and my husband: Dixit Reddy for their guidance, encouragement and unwavering support. I would also like to thank all my relatives and friends for giving me a wonderful experience during my stay here in LSU.

Table of Contents

List of Tables

List of Figures

Glossary

Acceleration: The rate of change of velocity. It is a vector quantity.

Biomechanics: Scientific study of living systems using physical principles.

Canter: A three-beat gait, with a footfall sequence (with a left fore lead) of right hind, then left hind with right fore, followed by left fore.

Center of mass: Point through which the weight of a body acts.

Distal: Away from the center of the body.

Elasticity: Ability of a body or material to resist deformation and to restore the original shape and size after it has been deformed.

Force: A measure of the action of one body on another that tends to change a body's state of rest or uniform motion in a straight line. It is a vector quantity.

Forward dynamics: It is a mathematical method to calculate the motion of the body based on known forces/torques.

Free body diagram: Diagram of a body completely free of its environment, with all the forces acting on it shown as vectors.

Ground reaction force: External force exerted by the ground on a body in contact with it.

Impulse: Function which has unit value only at time $t = 0$ and value is zero at time $t \neq 0$.

Impulse response: Output of any system for an impulse input.

Inverse dynamics: It is a mathematical technique to determine forces and moments needed to produce kinematic motions.

Joint reaction forces: the equal and opposite forces that exist between adjacent bones at a joint caused by the weight and inertial forces of the two segments.

Kinematics: Branch of classical mechanics that describes the motion of bodies and systems.

Kinetics: Branch of classical mechanics describing the forces involved in creating and changing motion.

Proximal: Towards the center of the body.

Stance phase: Part of the stride when hoof is in contact with the ground.

Stride: Complete cycle of limb movements during a gait.

Stride time: The period of time from one event (usually initial contact) of one limb to following occurrence of the same event with the same limb

Swing phase: Part of the stride when the hoof has no contact with the ground.

Trot: Two beat gait involving diagonal pairs of limbs. The right hind and left front move together, and the left hind and right front move together.

Walk: Symmetrical, four beat, stepping gait with a lateral footfall sequence. Horse's legs follow this sequence: left hind limb left front limb, right hind limb, and right front limb. At the walk, the horse always has one foot raised and the other three feet on the ground.

Abstract

Therapeutic horseback riding is a common component of physical therapy programs. Quantification of the horse back forces will provide vital information to match therapeutic riders with equine partners. To meet this medical need, a model to quantify the horse back forces from ground reaction forces was developed to test the hypothesis that the forces transferred to a static weight on the horse's back can be predicted given horse breed and weight. Simultaneous, real time kinetic, kinematic, and back force data on a static weight were collected from 7 adult horses: 3 thoroughbreds, 3 quarter horses, and 1 paso fino. An integrated system consisting of a force platform, an active motion detection system and wireless force transducers were used. Data was collected from a minimum of four successful trials from all horses at a walk (1.3-2.0 m/s). Inverse dynamic analysis was used to calculate the fore and hind limb joint forces to the shoulder and hip, taking into consideration all 4 limbs' motion per stride cycle. Virtual segments were created to model the equine back as a series of springs and dampers and joined to the limbs. Calculated forces from the inverse dynamics analysis were then input to the spring-damper model sequentially and at the same frequency as data collection. The energy absorption coefficients were derived by aligning the model output forces of the fore- and hind limb data with measured back forces. Horse back forces were simulated with different coefficients for each breed, and specifically for each horse. . Simulated results had a significant positive correlation ($r = 0.81 \pm 0.04$, $p < 0.001$) with forces measured directly on the back. The data from this investigation will contribute to mechanisms to predict forces experienced by the rider during horse motion to advance the science of therapeutic riding.

1. Introduction

Therapeutic horseback riding is a common component of physical therapy programs. The horse is used as a tool to provide the required forces to the rider. Physical forces and motion experienced by the therapeutic riding participant are transmitted through the horse back (Peham and Schobesberger 2004). Every individual who needs therapy has a specific set of needs for recovery. The amount of force is an inherent part of the exercises within each therapeutic regimen. As the participant improves, his or her needs will change. In therapeutic riding, improvement for the participant could limit the amount of benefits he can obtain from a given horse, and therefore he must be matched with a different horse for further treatment. The ultimate goal is to streamline and optimize the process of matching horse and rider to attain the most effective therapeutic results.

In order to improve horse-rider pairing, it is useful to build a database of horses from where the users can identify the horse necessary for the best therapeutic results. The database would contain the forces that the horse would transmit to the rider. Given that it is impractical to measure the forces exerted by each individual horse, a different method to predict or simulate the forces is necessary. These forces may vary based on the horse size, breed, gender, gait and functional forces from the riders themselves. Interactions between the horse and the rider comprise a complex system of coupled dynamic body motion, and it is necessary to assume that the dynamic functional forces from the rider will vary among participants. While the exact measurement of the forces between the horse and the rider is a complex problem, it is important to solve one part of the system to reduce the problem (Lagarde, Peham et al. 2005). This study was focused on solving the horse component of problem.

To simulate the horse back forces using varied horse data, a mathematical model of the horse needs to be developed. Inverse dynamic analysis is a mathematical method used to compute the joint reaction forces and moments based on ground reaction forces (GRFs) and kinematics of linked segments. Each segmental limb is treated as a single free body diagram with inputs from the distal segment and an output to the proximal segment. The hoof segment input comes from the GRFs. Previous studies have analyzed the GRFs and their transmission through the lower equine limb by applying a similar model and inverse dynamic analysis (Clayton, Hodson et al. 2000; Clayton, Hodson et al. 2001). Another study by C. Peham (Peham and Schobesberger 2004) used a force sensor mat to directly measure the horse back forces, but this study focused on developing a better model for the horse back only. While both the limbs and the horse back have been analyzed separately before, the nature of their connection has not been studied. The pathway between the limbs and back cannot be modeled as a series of rigid segments since the scapula of the horse is connected to the shoulder with muscle tissue and not a joint. To overcome this problem, the horse the horse back can be represented using virtual segments that model springs and dampers. A mathematical model needs to be used in order to appropriately simulate the horse back forces.

The forces exerted by a horse's back on a rider during motion are affected by the breed and weight of the horse. These forces are related to the ground reaction forces (GRFs), which can be measured using force platforms. The relationship however, has yet to be established. A prominent difficulty in establishing the relationship between the forces at the horse back and GRFs is due to the fact that there is no direct segmental connection between the equine back and the limbs (Phillips and Aspinall 2006). Since there is no direct connection, the GRFs cannot be used to directly solve for the back forces of the horse. Inverse dynamics has to be applied using

the mass, inertial properties, and acceleration of the horse limbs to calculate the forces that terminate at the scapula and hip. The analysis of the horse back brings forth more difficulties, since it has long back muscles that absorb and release energy; we have to assume that the back muscles do not change the forces being transferred. These forces are thus transferred through virtual segments consisting of springs and dampers onto the horse back. The back forces are then validated using data from customized force sensing equipment placed on horse back.

To relate the GRFs and horse back forces, we seek to construct a mathematical model that utilizes the horse breed, size, and weight to predict the forces at the back of the horse. In this study, the limbs were modeled as open-chain rigid body segments and the horse back was modeled as a series of springs and dampers. A mathematical model and a simulation module were developed to solve the equations of motion of the limb model, and compute appropriate spring and damper coefficients of the mechanical model of the horse back. This model has not been attempted before and should further the science of equine biomechanics in general. It also sets the foundation for future, more specialized and accurate equine models. A database developed using this model can streamline the process of pairing horse and rider for therapeutic riding.

2. Literature Review

2.1. Therapeutic Riding

The horse has been used as a therapeutic tool since at least the seventeenth century (Bliss 1997). More than 700 therapeutic riding centers accredited by the North American Riding for the Handicapped Association (NAHRA) exist in US and Canada. These centers assist with a wide range of disabilities including spinal cord injury, cognitive deficits, cerebral palsy, emotional disorder and amputation (Bertoti 1988; All, Loving et al. 1999). Horses provide neuromuscular stimulation through their movement. The three dimensional rhythmical moment of the horse is very similar to the action of the human pelvis; the horse's stride moves the rider's pelvis with the same rotation and side-to-side movement that occurs with walking (Lessick, Shinaver et al. 2006). This coupled rhythmical movement is utilized in various physical therapy programs (Hammer, Nilsagård et al. 2005).

One of the benefits of horseback riding for children with physical disabilities is the facilitation of normal equilibrium reactions in response to the pelvic movement of the horse (MacPhail, Edwards et al. 1998). At least one variable from balance, gait, spasticity, functional strength, coordination, pain, self-rated level of muscle tension, activities of daily living and health related quality of life is improved with horseback riding (Hammer, Nilsagård et al. 2005). Not only does it improve the physical conditions of the children, but also provides lots of enjoyment (MacKinnon, Noh et al. 1995; Lehrman and Ross 2001).

The amount of benefit an individual with a disability gains from horseback riding depends on various factors, such as the type and severity of disability as well as the match between horse and rider. In order to benefit a rider, the riding instructor must be able to choose a horse that will fit the individual's needs. As of now, the suitable horse is determined based on the best body type

and gait combination for the rider. It has always been desirable to determine the appropriate horse for each individual based on functional parameters of the horse and the rider. Unfortunately, there is no scientific method or algorithm to determine the best combination (Lessick, Shinaver et al. 2006).

2.2. Ground Reaction Forces and Limb Kinematics

Force platforms have been using from decades to measure ground reaction forces. The pattern and amplitude of the forces change from slow walk to canter in various breeds. Virtually all vertical force tracings are single peaked at all speeds, but for the slowest trials (<2 m/s) the hind limb vertical forces are double peaked. Fast speed range significantly affects the kinetic and timing parameters. Peak forces increase and stride duration decreases with speed. Equine forelimbs have greater peak vertical forces and impulses when compared with hind limbs (Biknevicius, Mullineaux et al. 2004). Breed differences also influence the force platform measurements in horses. Sound warmbloods load their limbs with more body weight than quarter horses and also warmbloods have higher peak vertical force (PVF) values than quarter horses(Back, MacAllister et al. 2007). In a sound horse, the ground reaction forces of left and right limb pairs are almost identical. The accelerations and velocities of each segment of right and left limbs are symmetrical within the stride cycle. The gait patterns of different horses of the same breed are also similar. The symmetry of the ground reaction force peaks and impulses of the vertical forces of contralateral limbs exceed 95 percent (Merkens, Schamhardt et al. 1986). A rider on the back affects the ground reaction force peaks of the horse. The cumulative increase in the weight of the overall system increases the vertical force peaks (Clayton, Lanovaz et al. 1999).

Sagittal plain kinematic events of all anatomical joints with respect to GRFs of forelimb and hind limb were explained by E. Hodson (Hodson, Clayton et al. 2001; Hodson, Clayton et al.

2010). Stance phases of hind limbs and forelimbs coincide just after initial contact. Vertical GRFs decrease during the tripedal stance period and increase towards the end of the stance and the angle-time graphs of the fetlocks coincide with the vertical GRFs of the limbs.

2.3. Forces and Net Joint Moments of the Fore and Hind Limbs during the Walk

Net joint moments of the forelimbs and hind limbs of walking horses were analyzed by H.M. Clayton (Clayton, Hodson et al. 2000; Hodson, Clayton et al. 2001). During the stance phase, the shoulder and fetlock have the highest net joint moments whereas the coffin joint has the lowest. During the swing phase, peak joint moments occur at the coffin joint and decrease gradually to the shoulder. Since there is no ground contact, the swing phase joint reaction forces (JRFs) were much smaller in magnitude than the stance phase JRFs. The fetlock acts as a spring to store and release energy, and the coffin acts as a damper. The elbow generates the energy required to maintain forward movement, while the shoulder supports the trunk (Colborne, Lanovaz et al. 1997; Clayton, Hodson et al. 2000). In the hind limb, the hip and tarsal joints are the main sites of energy generation, while the stifle joint absorbs energy throughout the walking stride. Tarsal and fetlock joints support the hip during stance and swing, respectively. The coffin joint acts as an energy damper during stance, whereas the stifle joint absorbs energy in the stance and swing phases(Colborne, Lanovaz et al. 1997; Hodson, Clayton et al. 2001). The upper limb is the main source of energy generation compared with lower during the stride.

2.4. Inertial Properties

The analysis of biomechanical models based on rigid body dynamics uses either inverse or forward dynamics. Both of these require a complete set of the inertial properties including mass, center of mass, and inertial tensor of various body segments. Segmental inertial data of living subjects can be estimated by two different methods. Using geometrical models, the shape of the

segments can be approximated and the inertial properties can be calculated from volume and density (van Gurp, Schamhardt et al. 1986; van den Bogert 1989). These models are very sensitive to measurement errors and do not perform well for several segments (van den Bogert 1989). The other category is regression models based on cadaver studies (Chandler, Clauser et al. 1975; Buchner, Savelberg et al. 1997). For accurate estimations based on such analyses, a sufficiently large database and a maximal similarity between the test object and original cadaver segments is required (Hinrichs 1985).

A complete set of three dimensional inertial properties of Dutch warmblood horses were determined to test the regression equations to the estimation of the center of mass, mass, and inertia in living horses (Buchner, Savelberg et al. 1997). Cadaver segments were separated at segment boundaries and mass, center of mass and density of each segment was found. Estimation of the segment mass, the total body mass (M) or the reference length (L) was used as an independent variable, while for the location of the center of mass (CoM), the reference length and axis components were used. It is impractical to use cadaveric segments of all horses to identify the inertial properties. Hence, the inertial data of Dutch warmblood horses is used as a reference for all the locomotion studies with different breeds (Clayton, Hodson et al. 2000; Hodson, Clayton et al. 2001).

2.5. Kinematics and Kinetics of Equine Vertebrae and Scapula Junction

There are several studies which provide the kinematic properties of equine vertebrae during the three horse gaits: walk, trot and canter. Kinematics of thoracic, lumbar, sacral vertebrae and tuber coxae were determined by the use of bone affixed (3D) and skin affixed markers (2D). There is a strong correlation between the results of 2-D and 3-D calculations in terms of flexion-extension (FE), abduction-adduction and lateral bending at both the walk and the trot. The direct

linkage between the hind limbs and vertebral column (i.e., sacroiliac joint) allows only a small amount of mobility. This limitation stems from the fact that the horse is quadruped, and although capable of rearing, rearing is not a component of normal gait and stance. An indication that flexion-extension is generated by the hind limbs comes from the pronounced shift in the timing of the minimum and maximum values (Faber, Schamhardt et al. 2000; Faber, Schamhardt et al. 2001).

P. Cocq (Cocq, Weeren et al. 2004) presented a study to find the influence of equipment and weight on the horse back kinetic and kinematic properties. This study concluded that there is no influence on any of the variables of the back measured at walk with surcingle or a saddle. However, overall extension of the back was increased by a 'saddle with 75 kg weight', which sufficiently simulate the saddle with a rider (Cocq, Weeren et al. 2004).

C. Peham (Peham and Schobesberger 2004) measured the exterior vertical forces on the horse back using a saddle sensor mat to investigate the internal forces and torques at horse back during different load scenarios of the equine back, such as with and without a rider. They reduced the complex anatomy of the equine back to two fundamental components: the vertebral column and the long back muscles. This simplified model consisted of 20 cylindrical segments, representing the thoracolumbar spine from thoracic vertebra T5 to lumbar vertebra L6, coupled to each neighboring segment with a central spherical joint and 4 springs. Model input consisted of the Electromyography (EMG) signal from the long back muscle and the load of the rider measured with the sensor mat. The resultant internal forces were computed using a built-in differential equation solver with variable step size optimized for mechanical multi-body simulation using ADAMS software and found that there was no change in maximal traversal forces with the rider at walk and trot (Cocq, Weeren et al. 2004; Peham and Schobesberger 2004).

An interesting fact is that the horse's shoulder is not attached to the spine by a collar bone as it is in humans. Instead, the shoulder is attached to and supports the weight of the front end by sheets of muscle. These sheets of muscle attach the shoulder blade from various points along the cervical vertebrae (bones of the neck), the thoracic spine, and to the ribs. As a result, the muscles attached to the shoulder are responsible for absorbing the concussion of the horse (Phillips and Aspinall 2006). When the horse travels forward, the middle and base of the scapula are pulled forward by muscles in the neck, bringing the foreleg forward, and thus slopes the upper part of the scapula slightly backwards as it is pulled by muscles behind the withers. As that leg becomes weight bearing during motion, the muscles along the back of the scapula that attach it to the ribs and thoracic spine pull the middle and base of the scapula backwards. These muscles play an important role in the forelimb movement of the horse.

2.6. Inverse Dynamic Analysis

Inverse dynamics is a primordial technique used in biomechanical and gait analysis. It is primarily used to calculate the net forces and torques involved in the kinematic motions, and through this kinetic data gain insight on the joint torques and power used by a biological body. Inverse dynamics is the preferred kinetic analysis method because it is non-invasive for the participant. Motion capture and force platform data are the information required to perform inverse dynamic analysis. The use of inverse dynamics involves several assumptions: body segments are rigid bodies, joints are frictionless, uniform mass distribution in bones, and joints only have one degree of freedom (in 2-dimensional case). There are various mathematical methods that accomplish the inverse dynamic analysis.

The classical method of inverse dynamic analysis uses the vectorial Newton – Euler method for computing the intersegment moments and forces (Apkarian, Naumann et al. 1989; Vaughan

1992; Janice and David 1995; Glitsch and Baumann 1997). The movement of each segment in 3D gait is assumed to have six degrees of freedom (three Cartesian coordinates and three angles of rotation). Functions of derivatives of joint angles are considered in the iterative Newton-Euler method. Coordinate transformations and inverse kinematics are applied to compute the crucial gait variable and joint angles. The problem of redundancy of the musculoskeletal system is resolved by inverse dynamics with classical Newton-Euler equations.

The Cartesian coordinate's method is another new approach for inverse dynamic analysis (Silva and Ambrósio 2002). In this approach, the anatomical body is defined by a rigid segment model. The joint between two adjacent segments is defined using an anatomical point and a joint direction unit vector (Silva, Ambrosio et al. 1997). In order to correctly represent the physical characteristics of the equine body, the principal physical properties of each anatomical segment such as mass, principal moments of inertia, segment length and center of mass (CoM) position must be specified. The position and orientation of a rigid body in the global reference frame are defined using the Cartesian coordinates of a set of basic points and direction unit vectors (De Jalon and Bayo 1994). In order to calculate the reaction forces and moments at the joints systematically, an expanded mechanical model that models the limbs and horse back are used. This model overcomes the rigid body constraints like maintenance of constant distances between pairs of points on a rigid body, constant angles between pairs of unit vectors, or between two-point segments and unit vectors (Silva and Ambrósio 2002).

The homogenous matrix method is also based on an iterative Newton–Euler formulation. It has the advantage of computing the moments and forces from simultaneous video and force platform data without requiring any assumption on the joint kinematics. To implement this method, a generalization of the homogeneous operator in dynamics was proposed by Legnani

(Legnani, Casolo et al. 1996). In this approach, mathematical operations are performed on three matrices: force platform measured ground/foot action matrix, gravity matrix and pseudoinertial matrix in order to compute the joint moments and forces (Doriot and Cheze 2004).

Conventional inverse dynamic methods yield separate computations of the forces and moments with successive coordinate system transformations. Body segment parameters are defined based on the assumption that the inertia tensor is the reference segment and the center of mass is located between the proximal and distal ends. 2D conventional methods can compute the net joint moment and forces of equine fore and hind limbs in the sagittal plane (Clayton, Hodson et al. 2000; Hodson, Clayton et al. 2001). In contrast, the 3D method uses Euler or Cardanic angles that are sequence dependent and suffer from singularities. Moreover, the conventional methods are not applicable for terminal segments as the GRFs are applied at the center of pressure instead of the segment distal end. Using wrench notation (Dumas, Aissaoui et al. 2004) overcomes these issues, where an optimized one step inverse dynamics method is used instead of the conventional three step approach (Apkarian, Naumann et al. 1989; Vaughan 1992; Janice and David 1995; Glitsch and Baumann 1997).The results of comparison among these methods reveal that the patterns and amplitudes of joint forces and moments are similar (Dumas, Nicol et al. 2005).

2.7. Biomechanical Structures of Living Animals as Springs and Dampers

Many mechanical and biomechanical structures can be modeled as a sum of spring and damper components. A dashpot in conjunction with a spring acts as a shock absorber and controls the movement. According to Hooke’s law, extension or compression of the spring is directly proportional to the applied load. The force exerted by the spring divided by the distance

it travels is defined as the spring constant. The spring constant defines the elasticity of the system, whereas damping coefficients determine the decay time of the oscillations of the system.

Mass and spring models have been used in various studies to characterize the biomechanical features of equine limbs and muscles (Lee, Koo et al. 1998). Viscous damping helps absorb shocks and limit from oscillations. Viscous damping and stiffness of the body can be quantified by dashpot-spring-mass models (Zhang, Xu et al. 2000).

Muscular control of the complex musculoskeletal system is based on the understanding of physical principles of musculotendon actuator action. The muscle is assumed to consist of two components: an active force generator and parallel passive component. The muscle's contractile element produces the active force and non-contractile contributes the passive. The passive component is assumed to include a parallel elastic element that represents the passive muscle elasticity and a damping component which corresponds to the passive muscle oscillations. The contractile element is parallel to the spring and damper to produce active force. The tendon attached to the muscle can be considered as a spring like structure which is in series with active and passive elements (Crowe 1968; Martin and Schovanec 1998; Erdemir, McLean et al. 2007).

3. Model Selection and Outline of the Study

Various models have been used in order to analyze the forces related to equine motion. H. M. Clayton (Clayton, Hodson et al. 2000; Clayton, Hodson et al. 2001) has applied biomechanical models and conventional inverse dynamics to analyze GRFs and calculate JRFs at the limbs. C. Peham (Peham and Schobesberger 2004) has modeled the horse back as springs and cylinders to determine how the rider's weight affects the horse back. The purpose of this study is to simulate the horse back forces of three breeds of horses. It is thought that applying a linked segment biomechanical model in conjunction with a series of springs and dampers will yield the horse back forces.

In order to develop a biomechanical model of the limbs and a mechanical model of the horse back, ground reaction forces, horse motion data, and horse back forces were collected at 200Hz simultaneously using three separate systems that were synchronized. To collect ground reaction forces, the horses were walked across a force platform which measures forces acting on its surface. Horse motion data was collected with a wireless motion capture system consisting of a series of 22 led markers attached to the left side of the horses at specific anatomical landmarks which generated a stick figure model of the horse. Horse back forces were measured with a wireless force sensing system and a custom modified equipment to hold a 12 kg lead weight in an aluminum box. Four wireless force sensors were placed under the four corners of the weight to measure the horse back forces.

The inertial properties of the limb segments were determined using published literature. The biomechanical model of the limbs was created by dividing the limbs into rigid link segments. The collected ground reaction forces, accelerations, and inertial properties were analyzed using the inverse dynamic approach. Inverse dynamic analysis is based on Newton-Euler equations

which computed the joint reaction forces at every joint up to the shoulder and hip. The joint reaction forces, which were only computed from the left side of the horse, were applied to the right side and adjusted for the horse's stride cycle to create a complete limb model of the horse.

The mechanical horse back model was composed of a series of springs and dampers. The algebraic sum of the joint reaction forces of all four limbs was applied to this mechanical model. The spring and damper coefficients were determined by systematically inserting the spring and damper coefficients into the equations until the output was within 10 N of the measured horse back forces.

4. Materials

4.1. Horses

The experimental protocol was approved by the Animal Care and Usage Committee of Louisiana State University, Baton Rouge, LA. Six clinically sound horses (One paso fino, three quarter horses and two thoroughbreds) and one lame thoroughbred from the Equine Health Studies Program were used in this study (Table 1). The age of the horses was 9.8±4.9 (Mean±SD) yr, mass was 488.2±73.2 (Mean±SD) kg and height, measured at the withers was 1.56±0.19 (Mean±SD) m. All the horses were housed in 1-acre separate pastures during the study.

Table 1: Weight, height, gender and age of thoroughbred, quarter horse and paso fino horses included in the study.

	Thoroughbred (TB)				**Quarter Horse (QH)**				**Paso Fino (Paso)**			
	Weight (kg)	*Height (m)*	*Age (years)*	*Gender*	*Weight (kg)*	*Height (m)*	*Age (years)*	*Gender*	*Weight (kg)*	*Height (m)*	*Age (years)*	*Gender*
H1	**576**	**1.7**	**9**	**Mare**	**454**	**1.5**	**18**	**Gelding**	**368**	**1.29**	**13**	**Gelding**
H2	**535**	**1.85**	**4**	**Gelding**	**541**	**1.42**	**10**	**Gelding**	**N/A**	**N/A**	**N/A**	**N/A**
H3	**431**	**1.67**	**4**	**Gelding**	**513**	**1.5**	**11**	**Gelding**	**N/A**	**N/A**	**N/A**	**N/A**

4.2. Force Platform

A force platform was used to measure the GRFs of the horses. It is an AMTI Model BP900900 force platform with a vertical capacity of 4450N (Advanced Mechanical Technology, Inc., Watertown, MA) (Figure 1). This force platform uses strain gages mounted on four precision strain elements to measure forces. AMTI's MSA-6 and DSA-6 amplifiers provide high excitation and amplification for multiple channels. It measures the three orthogonal force

components along the mediolateral (X), craniocaudal (Y) and vertical (Z) directions (motion) at a maximum of 800Hz. This study focused on the sagittal plane alone; therefore, craniocaudal and vertical forces were only used. This force platform was integrated to a wireless motion tracking system.

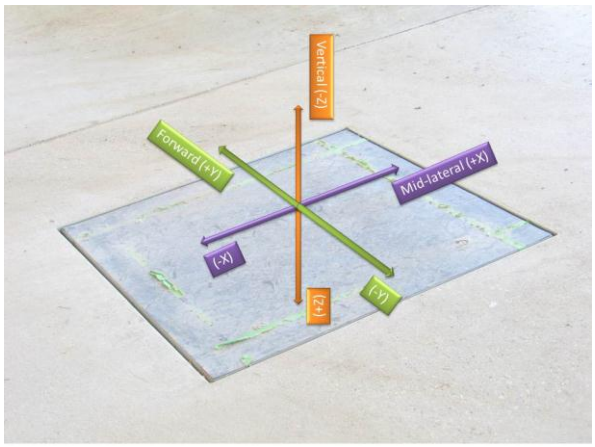

Figure 1: Force platform mounted on concrete runway to measure the ground reaction forces of large animals in mediolateral, craniocaudal and vertical directions.

4.3. Wireless Motion Detection System

- **Hardware**

A wireless motion system (Codamotion system, Codamotion Charnwood Dynamics Ltd, Leicestershire, UK) was used to track the horse's motion in terms of position, acceleration, velocity and joint angles at a sampling rate of 200 Hz with 22 infra-red LED markers. These LED markers were attached to the left side of the horse at 22 anatomical landmarks. This system used consists of two synchronized Codamotion Cx1 scanner units. Each Coda scanner contains three pre-aligned cameras to detect the position of a number of active infrared (IR) LED markers powered by drive-boxes (Figure 2). All the drive boxes contain a battery and sophisticated circuitry which responds to synchronizing infrared pulses sent out from the infrared light emitter at the Coda scanner units. The system flashes each marker and captures the infrared light from

each marker sequentially within each sample period, in order to generate one data set per sample. The motion detection data are sent to the host computer which is connected via a RS-422 serial port interface through an active hub (Figure 2). The active hub is used to provide a high speed serial communications link to the Coda scanner unit via the Coda interface cable and then to the host computer using a serial cable. It can support up to two Coda Cx1 scanner units. When the two Coda units are connected to a single hub, they are automatically synchronized (Codamotion).

(a)  (b) 

(c) 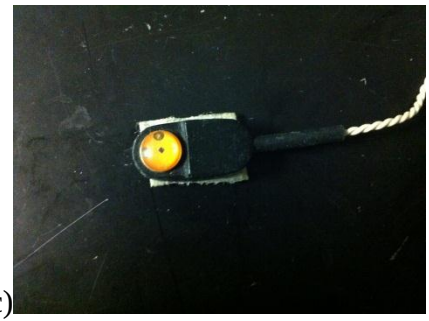 (d) 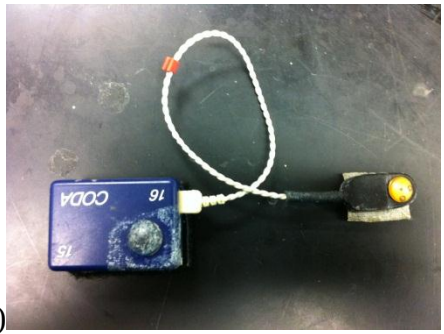

Figure 2: Codamotion system (Wireless active motion sensing system) a) Two Cx1 Scanners b) Active Hub c) Marker d) Driver Box.

Charnwood Dynamics claims the angular resolution of each camera is about 0.03 mrad (0.002 degrees) which results in a lateral position resolution of about 0.05mm at 3 meters distance (horizontally and vertically), and a distance resolution of about 0.3mm. The measurement

volume extends from a distance of 2.0m to about 6.0m in front of the measurement unit, at a width and height approximately 1.6 times the distance. These values are assumed to be at an ideal condition where the markers are not moving. The Codamotion manual and website do not specify at which conditions these values are applicable.

- **Software**

The Codamotion Analysis software provides the user-interface to the Coda hardware for real-time data display, data acquisition (marker position and ground reaction force), and also the data processing functions for analyzing the data (Figure 3).

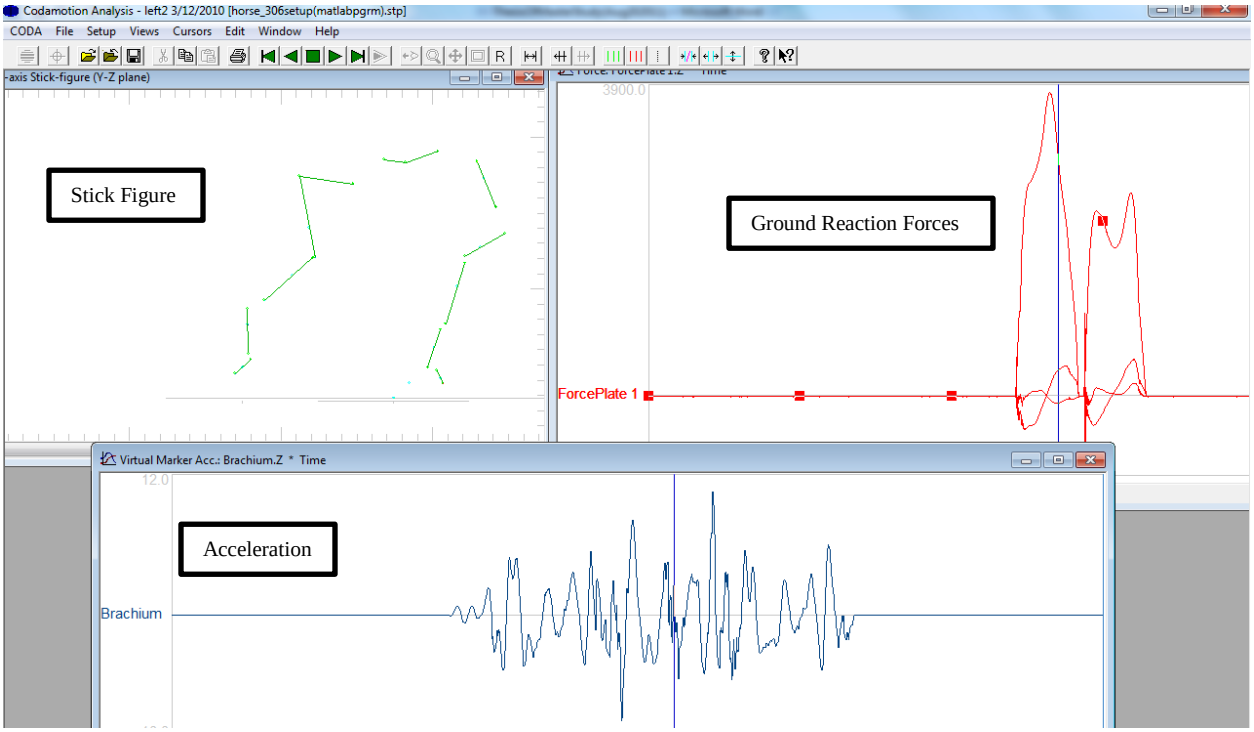

Figure 3: Codamotion platform with marker stick figure, ground reaction forces and marker acceleration.

4.4. Custom Force Sensing Equipment

Force sensing equipment was built to hold a lead brick of dimensions 8” x 4” x 2” and 12 kg weight on the back of a moving horse. The equipment allowed the weight to move only in the

vertical direction. Two surcingles of width 4” were held together using two PVC plates 15” wide x 10” long. One PVC platform was placed on and fastened to the surcingles with bolts. The second PVC platform was placed on top of the first. To prevent injury to the horse, a foam pad was glued between the bolt heads and the horse back with a leather patch. An open top-

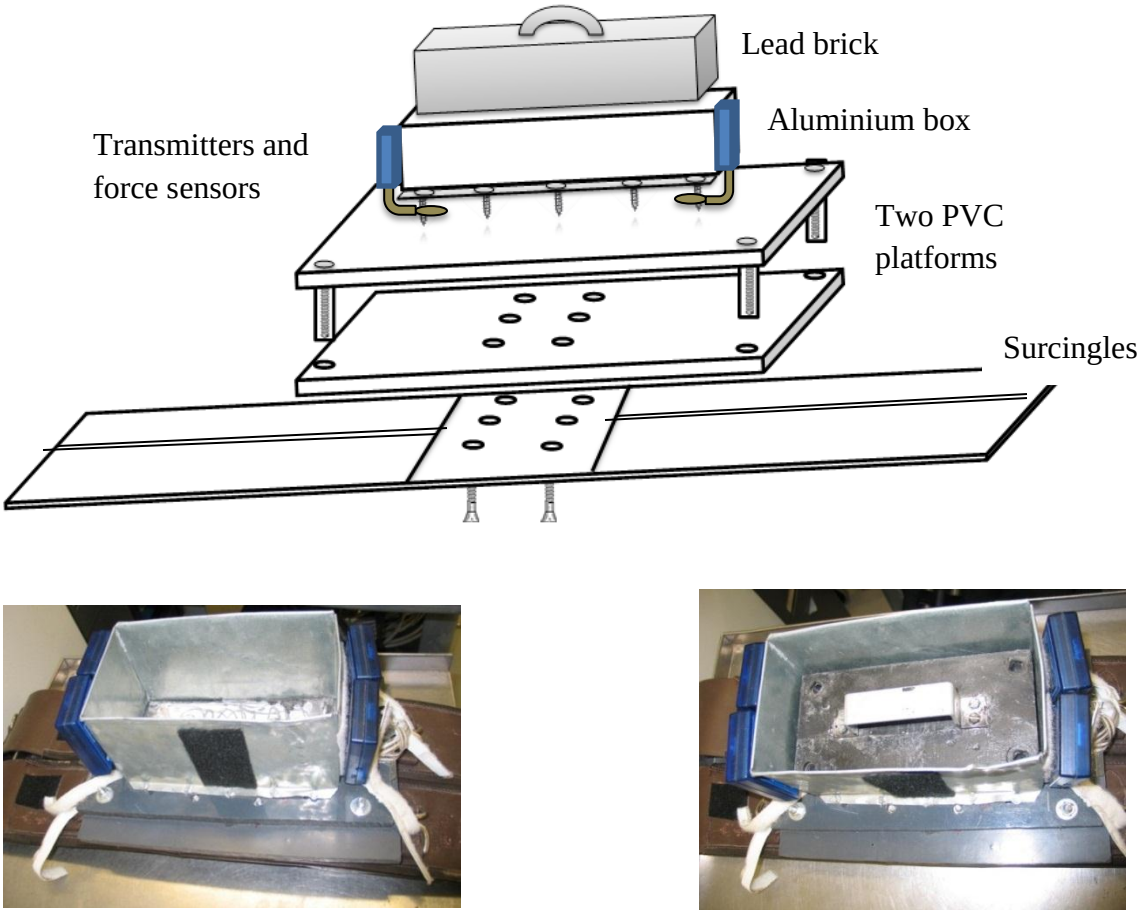

Figure 4: Schematic of custom force sensing equipment with and without weight.

-aluminium box of size 8 ¼”x4 ¼” was affixed to the top PVC sheet with a series of small bolts. A handle was attached to the top of the lead weight so that the weight could be moved in and out of the aluminium box with ease (Figure 4). This customized system is used to measure the forces from the horse back on a 12 kg weight.

4.5. Wireless Force Sensing System

A wireless force sensing system (Wireless Economic Load and Force System, Tekscan Inc.) was used to measure the horse back forces due to 12 kg lead weight. Each ELF system consists of wireless ELF software, transmitter, receiver, and flexible force sensors (Figure 5). The application of force to the active sensing area of the sensor results in a change in the resistance of the sensing element in inverse proportion to the force applied. Force sensors with a 1" diameter and a range of 0-111 N were used to measure the static forces (Tekscan). The transmitter, which is connected to the flexi force sensor, sends a signal to the receiver which is connected to a computer through a USB hub. After a simple calibration, the force is recorded in Newtons (Tekscan).

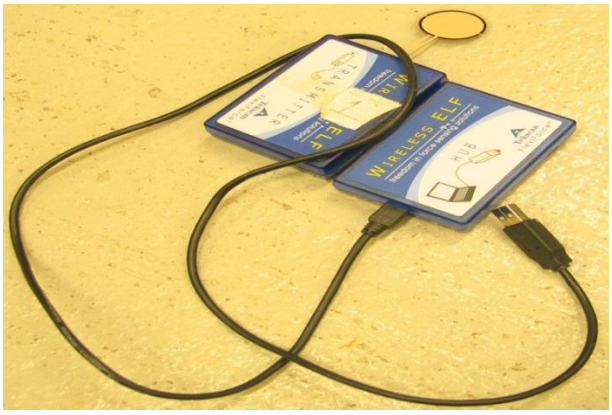

Figure 5: Wireless ELF system (Force sensors, Transmitter and Receiver) is used to measure the static forces.

The ELF software allows the user to view a graphical representation of the force on each sensor in real-time, record this information as a series to review and analyze it later. The data was displayed as a strip graph in the software and later saved as ASCII files to import into Microsoft Excel(Tekscan).

4.6. Double Mouse

The motion detection system and force platform were integrated into one host computer and synchronized with a proper configuration and setup files. A double mouse was built to synchronize the force sensing system with the other two by starting data collection on all the systems with only one mouse click (Figure 6). A double pole switch was connected to both Ps/2 mouses to turn them ‘ON’ simultaneously. One end of the USB adapters from the mouses was connected to the serial cables from the mouses and the opposite ends were connected to the computers one of which had Codamotion software (Codamotion) and the other Tekscan software (Tekscan ; Tekscan ; Tekscan). A double pole switch “ON” was used to trigger a mouse left click on both systems simultaneously.

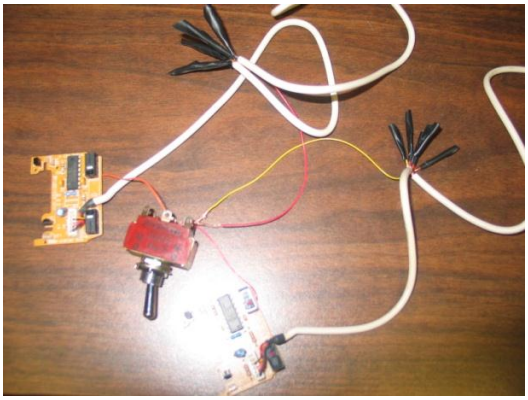

Figure 6: A double mouse composed of two mouses and one double pole switch. Active and ground pins of both the mouses were connected to the corresponding pins in the double pole switch to activate both the mouses with double pole switch.

5. Methods

5.1. Data Collection and Retrieval

The horses were trained to walk over the force platform prior to data collection. The infrared LED markers were attached to the clipped skin of each animal by adhesive velcro over twenty-two anatomical landmarks on the left forelimb, back, and left hind limb as described in the literature(Clayton, Hodson et al. 2000; Clayton, Schamhardt et al. 2000; Hodson, Clayton et al. 2001): 1) Proximal hoofwall on distal interphalangeal joint, 2) Proximal P3, 3) Metacarpal attachment of lateral collateral ligament (LCL), 4) Head of fourth metacarpal bone, 5) Ulnar carpal bone, 6) Radial insertion of LCL, 7) Lateral epicondyle of humerus at LCL, 8) Greater tubercle of the humerus, 9) Distal aspect of scapula, 10) Proximal aspect of scapula 11) Withers, 12) 12^{th} thoracic vertebra, 13) 18^{th} thoracic vertebra, 14) Tuber coxae, 15) Femoral greater trochanter, 16) Femoral origin of lateral patellar ligament (LPL) 17) Tibial insertion of the lateral patellar ligament(LPL), 18) Lateral malleolus, 19) Head of the 4^{th} metatarsal bone, 20) Metatarsal origin of LCL 21) Metatarsal attachment of the lateral patellar ligament(LPL) of the fetlock and 22) Rear proximal hoof wall over the distal interphalangeal joint(DIJ)(Figure 7). The drive boxes were attached in the middle of each segment with adhesive velcro, between the markers. The Coda sensors were connected to the active hub on the host computer through the serial port. These two Cx1 sensors were kept 2m apart to capture the motion of the horse on at least 15m of runway and across the force platform. The horse was then positioned motionless in front of the Cx1 sensors in order to confirm all markers were working and being captured by the system. The data flowchart is shown in Figure 8.

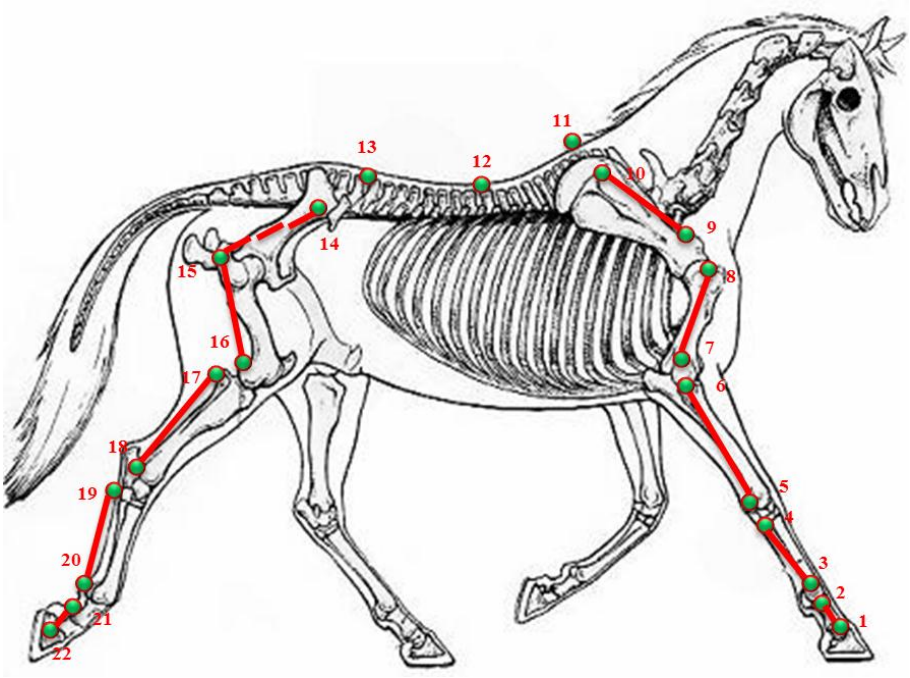

Figure 7: Location of infrared markers and connecting stick figure.

Horses were walked across the force platform at 1.2 – 2.0 m/s by a trained handler. Data was collected under three different conditions: 1) No equipment, 2) Surcingle only, 3) Surcingle box containing 12kg weight (Figure 9). In the third condition, four force sensors were placed under the weight at each corner to measure the horse back forces. The force sensors were calibrated with a mechanical testing system (Instron Dynamight 8841). The system was calibrated according to the manufacturer's calibration procedure. First, the calibration module is initialized in the Wireless ELF software. A mass of 0.5, 1, 2 and 5 Kg was applied sequentially to the force sensors using the Instron machine. A curve was then fitted in the calibration module to complete calibration. The double mouse was used to activate data collection in motion detection system embedded with force platform and the force sensing system at the same time. The wireless force sensor's receiver collected the force signals from the force sensor transmitter attached to the aluminium box. The signals of the force platform and LED markers were transmitted to the host computer. In a successful trial, fore hoof followed by the ipsilateral hind hoof landed entirely on

the force platform, with only one hoof contacting the force platform at a time. Trials that didn't meet the criteria were discarded. A minimum of four trials per side were collected for analysis. The GRFs and horse motion data in terms of marker position, velocity and acceleration were imported into Excel spreadsheets.

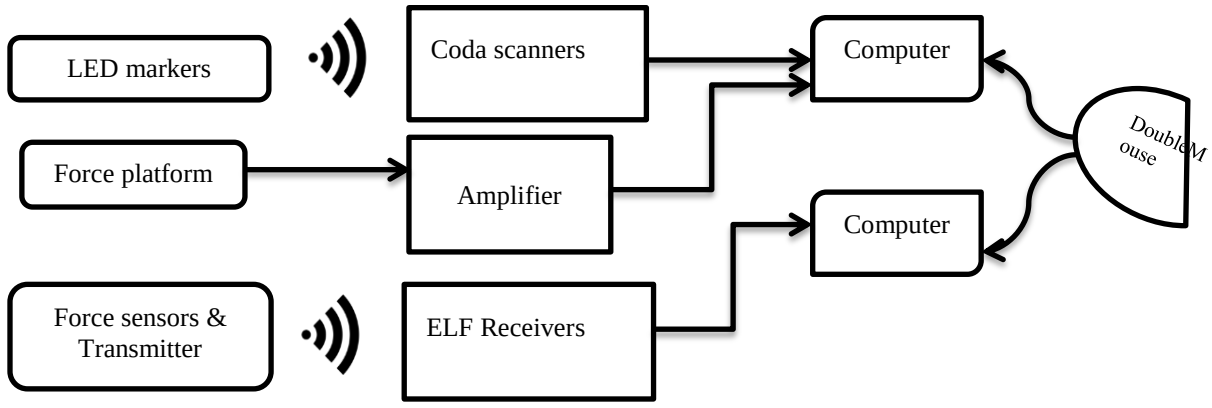

Figure 8: Block diagram of the data transfer from the force platform, motion detection system and force sensing system.

To reduce the discrepancies of motion of skin with respective to skeletal landmarks, the length of each segment was computed by taking the root mean square value of the distance between the markers of each segment over a stride cycle (Bobbert, Gómez Álvarez et al. 2007). The position of the center of mass (CoM) of each segment was represented with a virtual marker. The position of the virtual marker of each segment was computed using physical ratios obtained from the Dutch warmblood horses (Buchner, Savelberg et al. 1997) and compiled in MATLAB2010a. The acceleration of the virtual marker was obtained from the Codamotion software, and considered as the segment acceleration.

(a)  (b) 

(c) 

Figure 9: Pictures of all 3 conditions: a) No equipment; b) Surcingle only; c) Surcingle with 12kg weight inside the box.

5.2. Data Interpolation

Data from four flexi force sensors was interpolated to create continuous data from discontinuous. The results of the measurements were placed in a 2x2 matrix to represent the actual placement of the sensors. A virtual 4x8 matrix can be derived using appropriate ratios (Figure 10).

The virtual forces were derived using the following formulas:

$S_{k,i} = \frac{(j-1)S_{1,k}+(i-1)S_{4,k}}{(j-1)+(i-1)}$ for $k = 1,7; (i,j) = (1,4),(2,3),(3,2),(4,1).$

$$S_{i,k} = \frac{(j-1)S_{k,1} + (i-1)S_{k,7}}{(j-1)+(i-1)}$$

for $k = [1,4]; (i,j) = (7,2),(6,3),(5,4),(4,5),(3,6),(2,7).$

$$S_{total} = \sum_{i=1}^{4} \sum_{j=1}^{8} S_{i,j}$$

$S_{i,j}$ is the individual sensor force of the i[th] row's and j[th] column's sensor. S_{total} is the derived total horse back force due to 12kg weight. The virtual sensors are assumed to have a square area to take into account the entire force under the surface of the lead brick. The area under the circular sensors was approximated with the area of a square by multiplying by a scaling factor of $\frac{4}{\pi}$.

This technique is used for data interpolation from small samples. It is more appropriate if the data is acquired at each individual point. This study however, is considering the cumulative force at a single point which is easily computed by adding the real force sensed data from four sensors and multiplying with the scale factor $\frac{32}{\pi}$ (area under the brick is 8 x 4).

$$S_{sum} = S_1 + S_2 + S_3 + S_4$$

$$S_{total} = S_{sum} \frac{32}{\pi}$$

S_1 , S_2, S_3 and S_4 are measured forces from four sensors. S_{total} is the derived total back force under the 12 kg weight.

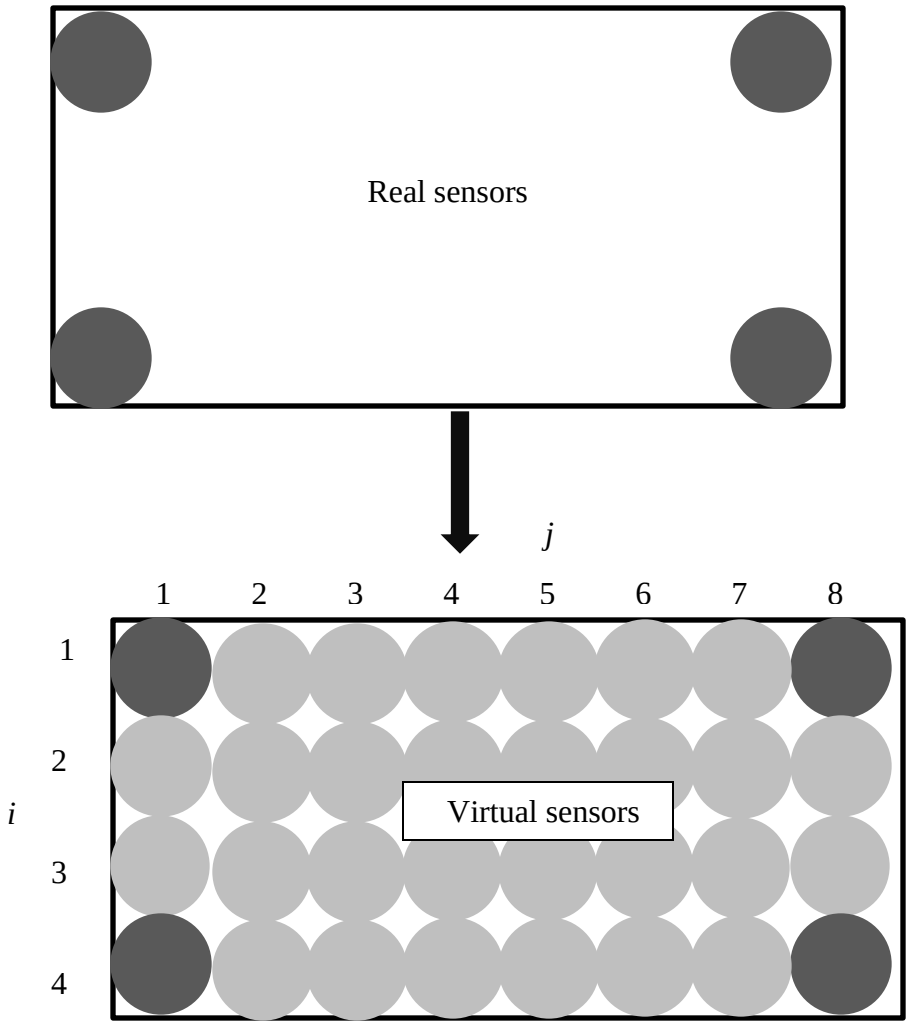

Figure 10: Virtual matrix derivation from real matrix.

5.3. Biomechanical Model to Quantify the Forces

A biomechanical model of the limbs in series with a mathematical model of the back is developed to derive the mathematical relationship between the GRFs and the horse back forces. A sagittal, two dimensional, symmetric horse model is constructed as a series of rigid links (Figure 11). Fore- and hind limbs are modeled as 5 and 4- rigid open chain links to the level of shoulder and hip, respectively. The back is modeled as a series of spring and damper components which are located over virtual segments. Forces from the neck and the head are not considered.

Kinematic data, GRF and inertial properties of limb segments are used to calculate net joint reaction forces (Buchner, Savelberg et al. 1997). Since it is not practical to directly measure mass and Center of Mass(CoM) position of each segment from the horses used in this study, mass and CoM components were determined from the published data based on the assumption that segment mass, CoM position and length of the experimental horses were proportional to the horses used for the published study according to the following formula (Buchner, Savelberg et al. 1997; Clayton, Hodson et al. 2000; Hodson, Clayton et al. 2001).

$$\boldsymbol{m_i^c} = \boldsymbol{m_i^{ref}} \frac{\boldsymbol{M_c}}{\boldsymbol{M_{ref}}},\ i = 1,2,3,....9$$

$$\boldsymbol{CoM_x^c} = \boldsymbol{CoM_x^{ref}} \frac{\boldsymbol{L_i^c}}{\boldsymbol{L_i^{ref}}},\ i = 1,2,3.....9$$

$$\boldsymbol{CoM_y^c} = \boldsymbol{CoM_y^{ref}} \frac{\boldsymbol{L_i^c}}{\boldsymbol{L_i^{ref}}},\ i = 1,2,3.....9$$

$$\boldsymbol{CoM_z^c} = \boldsymbol{CoM_z^{ref}} \frac{\boldsymbol{L_i^c}}{\boldsymbol{L_i^{ref}}},\ i = 1,2,3.....9$$

Where m_i^c and L_i^c are the mass and length of i^{th} segment sample horse. m_i^{ref} and L_i^{ref} are the mass and length of i^{th} segment of reference. M_{ref} and M_c are the total masses of reference and current horses, respectively. CoM_x^{ref} , CoM_y^{ref} and CoM_z^{ref} are the x, y, and z components from segment distal end to CoM position of the reference horse whereas CoM_x^c , CoM_y^c and CoM_z^c are the x, y, and z components from segment distal end to center of mass position of the currently using horse. CoM x, y, and z components of each segment were used to point the virtual markers in the Codamotion software in order to obtain segment accelerations. Virtual marker acceleration was considered as the segment acceleration.

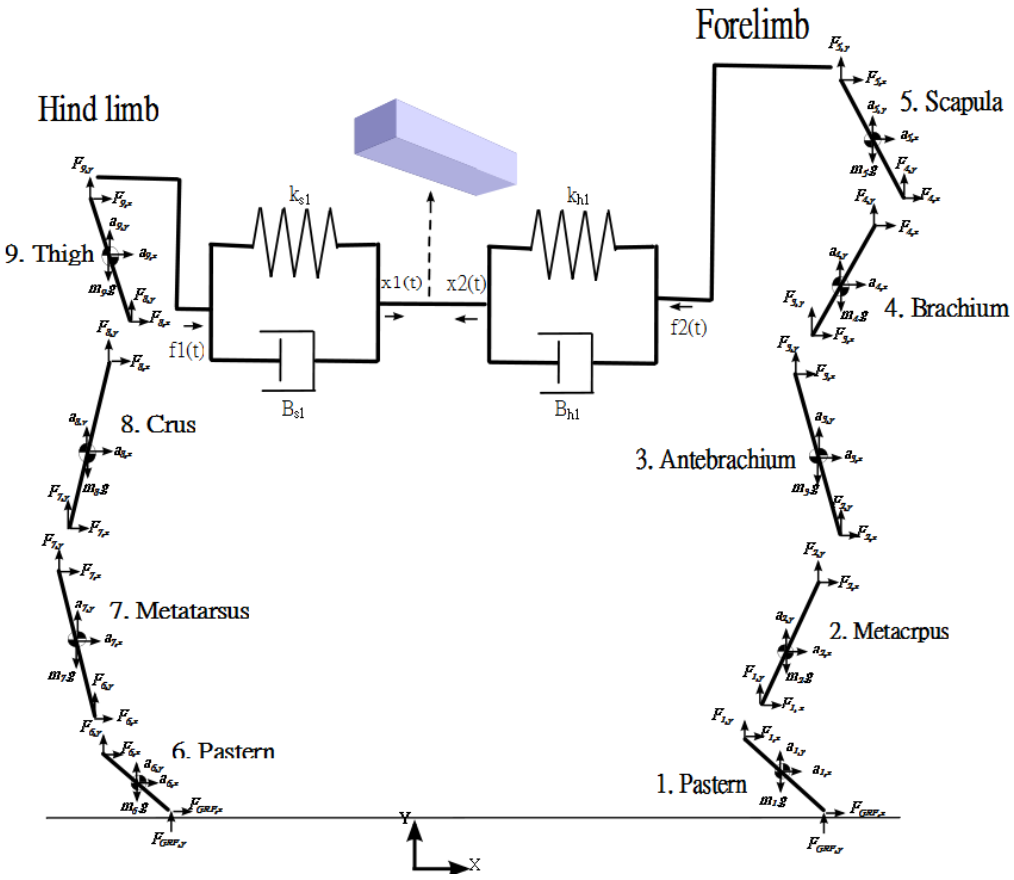

Figure 11: Combined biomechanical and mathematical models of the horse. All the segments of both the limbs to the level of the scapula and thigh are modeled as nine rigid open chain links with segmental inertial properties and the rest of the body is modeled as a sum of spring and damper components.

The transferred forces from ground to shoulder and hip joint are computed at the rate the data was collected over a complete stride cycle through inverse dynamic calculations. The joint reaction forces of fore and hind limb segments are computed for 5 and 4-rigid open chain-link models, respectively. The conventional 2D inverse dynamic method (Figure 12a) is applied to the model by utilizing 2nd order Newton-Euler formulation recursively in the sagittal plane (Vaughan 1992). Measured ground reaction forces are combined with the acceleration values virtual marker accelerations and inertial properties of each segment.

$$F_{i,y}(t) = \begin{cases} m_i^c a_{i,y}(t) - F_{GRF,y}(t), & i = 1,6 \\ m_i^c a_{i,y}(t) + F_{i-1,y}(t), & i = 1,2 \ldots . 9, i \neq 1,6 \end{cases}$$

$$F_{i,z}(t) = \begin{cases} m_i^c a_{i,z}(t) - F_{GRF,z}(t) + m_i^c g, & i = 1,6 \\ m_i^c a_{i,z}(t) + F_{i-1,z}(t) + m_i^c g, & i = 1,2 \ldots . 9, i \neq 1,6 \end{cases}$$

and, $$F_{i,net}(t) = \sqrt{F_{i,y}(t)^2 + F_{i,z}(t)^2}$$

$F_{i,y}$ and $F_{i,z}$ are the forward and vertical joint reaction forces and accelerations of i^{th} segment. $a_{i,y}$ and $a_{i,z}$are the forward and vertical accelerations of i^{th} segment. $F_{GRF,y}$ and $F_{GRF,z}$ are the forward and vertical ground reaction forces(GRFs). $F_{i,net}$ is the net joint reaction force at the i^{th} segment. The vector amplitude of forward and vertical force component is considered to get the net JRF amplitude. $F_{i,net}$ is the resultant joint reaction force due to vertical and forward components of the i^{th} segment.

For example, to begin an inverse dynamic analysis, the external forces at the terminal segment must be known. Once these forces are determined, a free body diagram must be constructed on a rigid body segment representative of the actual anatomical segment. This free body diagram should contain all the anatomical forces within the segment, i.e. weight at the CoM, and the external forces at the terminal point of the segment. A new free body diagram is now constructed that simplifies the anatomical forces into one net force, and also simplifies the external forces. The net anatomical force should be drawn about the proximal end of the segment, and the net external force should be drawn about the distal end of the segment that is in contact with the external forces. To obtain the magnitude and direction of these net forces, the corresponding component forces are added together. The net anatomical force is unknown but can be solved for by knowing the CoM, weight, and external forces on the limb. Once the net anatomical force is

calculated, it can be applied as the 'external force' for the following segment, and the process repeated (Figure 12b).

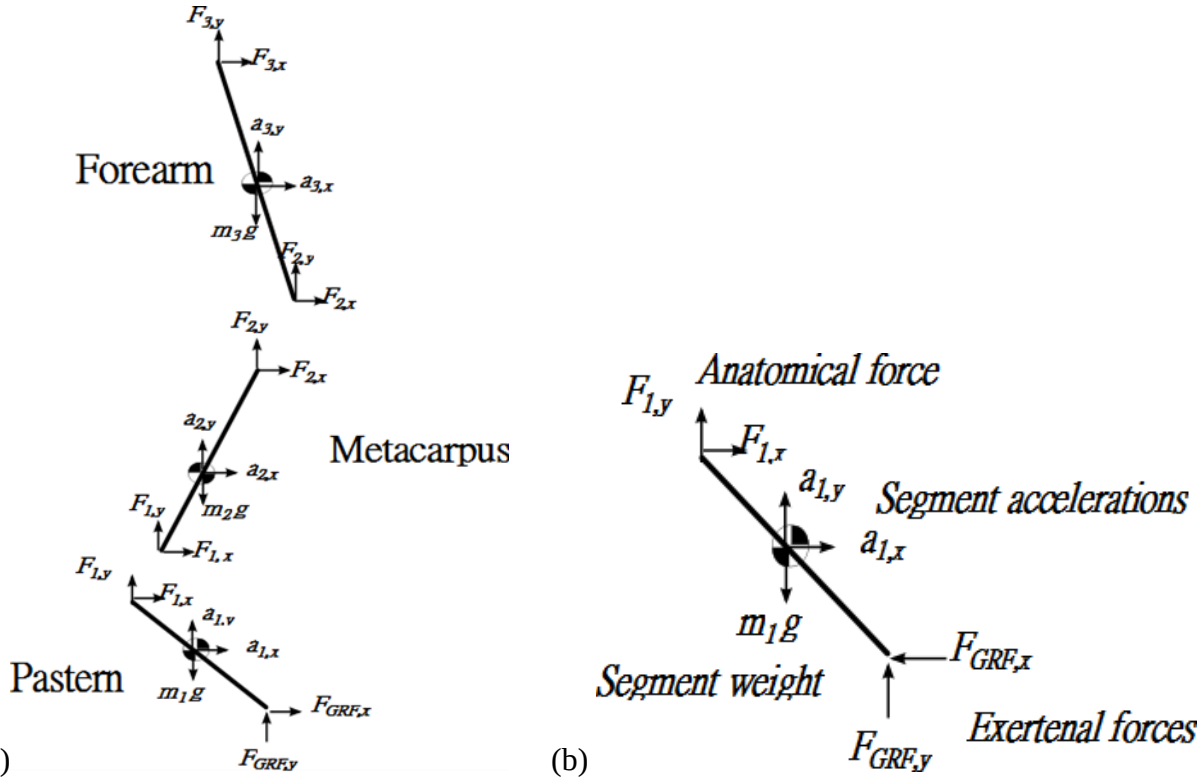

(a) (b)

Figure 12: Inverse dynamic rigid link model. (a) Rigid open chain link model of pastern, metacarpus and the forearm of the horse; (b) Free body diagram of Pastern

It is assumed that horse is symmetrical in the sagittal plane. The foot fall sequence at walk over a stride cycle is as follows: left forelimb, right hind limb, right forelimb and left hind limb and the stance phase of each limb occupies 62.5% of total stride cycle. The computed net JRFs at left side limb segments were applied to the right side limb segments and adjusted for the horse's stride cycle to create a complete horse limb model.

It is assumed that the horse back is a rigid body with 2 degrees of freedom (2-DOF). The axial rotation (roll) of the back is the absolute difference between the position of left and right limbs. The flexion and extension (pitch) is the absolute difference between back position for front and

hind limbs. This 2-DOF of horse back can be represented by taking the absolute difference of front and back spring-damper system outputs for left and right shoulder and hip JRFs.

The net JRFs over a stride cycle are fed to the spring-damper are fed to the spring The net joint force at the left shoulder joint $f_1(t)$ is applied to the spring in parallel to the damper model (Figure 13). The resultant displacement of the spring is $x_1(t)$. The system equations and transfer function of the system can be modeled as below with spring and damper coefficients k_{s1} and b_{s1}.

$$f_1(t) = k_{s1}x_1(t) + b_{s1}\frac{d\,x_1(t)}{dt}$$

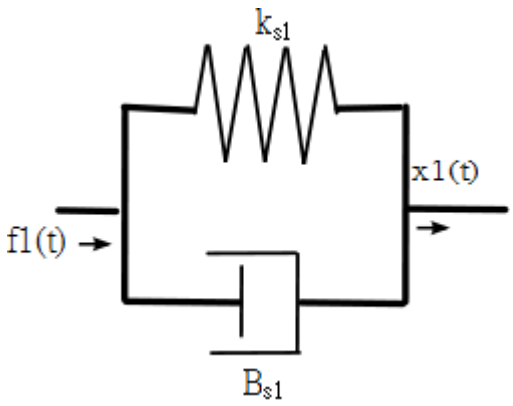

Figure 13: Spring and damper system with the coefficients k_{s1} and b_{s1}

Apply Laplace transform on both sides to get the system transfer function

$$£\{f_1(t)\} = £\left\{k_{s1}x_1(t) + b_{s1}\frac{d\,x_1(t)}{dt}\right\}$$

$$F_1(s) = k_{s1}X_1(s) + b_{s1}sX_1(s)$$

$$F_1(s) = X_1(s)(k_{s1} + b_{s1}s)$$

System transfer function $\frac{X_1(s)}{F_1(s)} = H_1(s) = \frac{1}{(k_{s1} + b_{s1}s)}$

Apply inverse Laplace transform to get final displacement

$$x_1(t) = f_1(t) * £^{-1}\{H_1(s)\}$$

$$x_1(t) = f_1(t) * e^{\frac{-k_{s1}}{b_{s1}}t} / b_{s1}$$

For the force $f_2(t)$ from the left hip joint applied to another spring-damper system results the displacement $x_2(t)$. The system equation and transfer functions are same as the first system with different spring and damper coefficients, k_{h1} and b_{h1} respectively. The displacement $x_2(t)$ can be written as

$$x_2(t) = f_2(t) * \mathcal{L}^{-1}\{H_2(s)\}$$

$$x_2(t) = f_2(t) * e^{\frac{-k_{h1}t}{b_{h1}}} / b_{h1}$$

Where $\frac{X_2(s)}{F_2(s)} = H_2(s) = \frac{1}{(k_{h1} + b_{h1}s)}$

If the stride time with respect to the left forelimb is T, then $x_1(t \pm T/2)$, $f_1(t \pm T/2)$, $x_2(t \pm T/2)$ and $f_2(t \pm T/2)$ are the applied force and displacement of the system for right front and rear of the horse. The resultant peak-to-low force $f_{p\_l}(t)$ on to the weight at the horse's back can be obtained by

$$x_f(t) = \left| f_1(t) * e^{\frac{-k_{s1}}{b_{s1}}t} / b_{s1} - f_1(t - T/2) * e^{\frac{-k_{s1}}{b_{s1}}t} / b_{s1} \right|$$

$$x_h(t) = \left| f_2(t) * e^{\frac{-k_{h1}t}{b_{h1}}} / b_{h1} - f_2(t - T/2) * e^{\frac{-k_{h1}t}{b_{h1}}} / b_{h1} \right|$$

$$f_{p\_p}(t) = \left| x_f(t) - x_h(t) \right|$$

$$f_{p\_l}(t) = \left| \left| f_1(t) * e^{\frac{-k_{s1}}{b_{s1}}t} / b_{s1} - f_1(t - T/2) * e^{\frac{-k_{s1}}{b_{s1}}t} / b_{s1} \right| - \left| f_2(t) * e^{\frac{-k_{h1}t}{b_{h1}}} / b_{h1} - f_2(t - T/2) * e^{\frac{-k_{h1}t}{b_{h1}}} / b_{h1} \right| \right|$$

The cumulative force on any weight is the summation of the weight (offset) and 'peak-to-low' (p_l) force. The offset force can be computed as follows:

Left shoulder joint JRF $f_1(t)$ is applied to the system transfer function $H_{1offset}(s)$ to get the offset displacement $x_{1offset}(t)$.

Where

$$H_{1offset}(s) = \frac{1}{(k_{s2} + b_{s2}s)}$$

and

$$x_{1offset}(t) = f_1(t) * \mathcal{L}^{-1}\{H_{1offset}(s)\}$$

$$x_{1offset}(t) = f_1(t) * e^{\frac{-k_{s2}}{b_{s2}}t} / b_{s2}$$

In the similar manner left hip side transfer function and displacements can be written as

$$H_{2offset}(s) = \frac{1}{(k_{h2} + b_{h2}s)}$$

and

$$x_{2offset}(t) = f_1(t) * \mathcal{L}^{-1}\{H_{2offset}(s)\}$$

$$x_{2offset}(t) = f_1(t) * e^{\frac{-k_{h2}}{b_{h2}}t} / b_{h2}$$

Offset

$$f_{offset}(t) = x_{1offset}(t) + x_{2offset}(t) + x_{1offset}(t \pm T/2) + x_{2offset}(t \pm T/2)$$

Where $x_{1offset}(t \pm T/2)$and $x_{2offset}(t \pm T/2)$ are right shoulder and hip side displacements.

$$f_{offset}(t) = f_1(t) * e^{\frac{-k_{s2}}{b_{s2}}t}/b_{s2} + f_1(t) * e^{\frac{-k_{h2}}{b_{h2}}t}/b_{h2} + f_1(t \pm T/2) * e^{\frac{-k_{s2}}{b_{s2}}t} / b_{s2} +$$

$$f_1(t \pm T/2) * e^{\frac{-b_{h2}k_{h2}}{b_{h2}}t} / b_{h2}$$

The resultant force on the weight is:

$$f_r(t) = f_{offset}(t) + f_{p\_l}(t)$$

5.4. Simulation of the Program

A schematic of the computer model for forces at the horse's back is given in the figure below. As shown in the Figure 14, the entire model is composed of four parts: i) User input, and GRF and locomotion data; ii) Inertial properties and inverse dynamic calculations; iii) Simulation; and iv) Horse back forces as output. The inputs, the main stages of the program, the simulation model and the outputs are explained in detail.

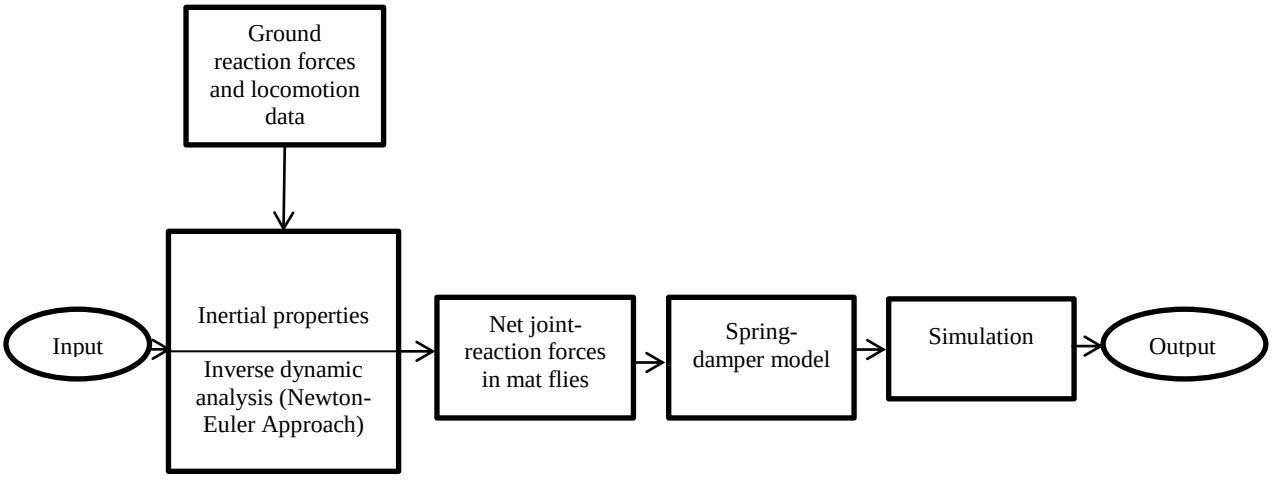

Figure 14: Schematic of the computer program to estimate the spring and damper coefficients for a given horse.

The user inputs to the computer program are the horse's name, mass and the filename from where the horse's breed, gait, ground reaction forces and kinematic data can be read. Horse's inertial properties are calculated using reference Dutch warmblood horse's data within the computer program. All of the inputs mentioned above have direct impact on joint reaction forces and horse back forces as inverse dynamic equations are functions of horse's mass and horse's locomotion data.

The program consists of script programming and graphical programming. In the script programming, the equations which describe the horse limbs' open chain rigid link model are formed. As described previously, conventional 2-D Newton-Euler is used to develop the inverse dynamic equations. These equations are second order nonlinear ordinary differential equations describing horse locomotion in terms of joint forces resulting from horse locomotion. Horse inertial properties such as mass and center of mass of limb segments are calculated in the program as described above. When the program is called from within MATLAB prompt, it asks from user to provide answers to the following questions.

- ✓ Enter the mass of the horse [kg]
- ✓ Enter the file name where kinematic data is stored [filename.xlsx]
- ✓ Enter the trial number

The resultant joint reaction forces of left fore- and hind-limbs are displayed graphically at this stage and stored in separate files. It is assumed that the left and the right side locomotion of the horse is symmetric over a stride cycle in terms of GRF and locomotion at the walk. Right limbs joint reaction forces are computed using symmetry. The four joint reaction force information files of the shoulder and hip on both sides are fed to a physical spring - damper model of the program. This model is developed using graphical programming using MATLAB Simulink2010a.

The block diagram of the model is shown in Figure 15. Built-in transfer function modules are implemented in Simulink to process the data obtained from the inverse dynamic analysis. The modules can be customized to simulate springs and dampers by inputting the appropriate k and b values into the transfer function. The transfer functions are manually optimized within a reasonable range for the anatomical position of the simulated spring-damper system. Spring

coefficients, k, from 10-200N/m and 100-800N/m are tested for the forelimbs and hind limbs respectively. Damper coefficients, b, from 0.01 to 10Ns/m are tested for all transfer functions. Only the spring coefficients or the damper coefficients are tested at any time, that is, one of the coefficient sets is kept constant while the other is changed until the desired result is obtained. The simulated graph is compared with the measured results graph for accuracy with every combination of k and b values. After a suitable combination of k and b values is found, the results are varied in the same manner in order to find a suitable range of values. The value range is found suitable if the number of peaks in the simulated graph remains the same as in the measured results graph and the upper and lower limits do not vary more than 10 N. During the simulation all the results from the second stage are displayed on the screen as plots. To obtain the impulse response, a unit impulse is applied to the system with a built-in Simulink pulse generator. When this impulse response is convoluted with the input data, the simulation results graph is obtained.

The outputs of the program are shown in the form of on-screen data and graphs. These outputs are listed as inertial properties of each segment of the limbs and joint reaction forces at the level of scapula and pelvis and simulated forces on the horse back.

5.5. Statistical Analysis

All the variables presented in this study are represented with mean±s.d. Linear correlation coefficient(r) of measured and simulated horse back forces was computed with Pearson's correlation test using GraphpadPRISM4.00 software (Graphpad software, CA, USA).

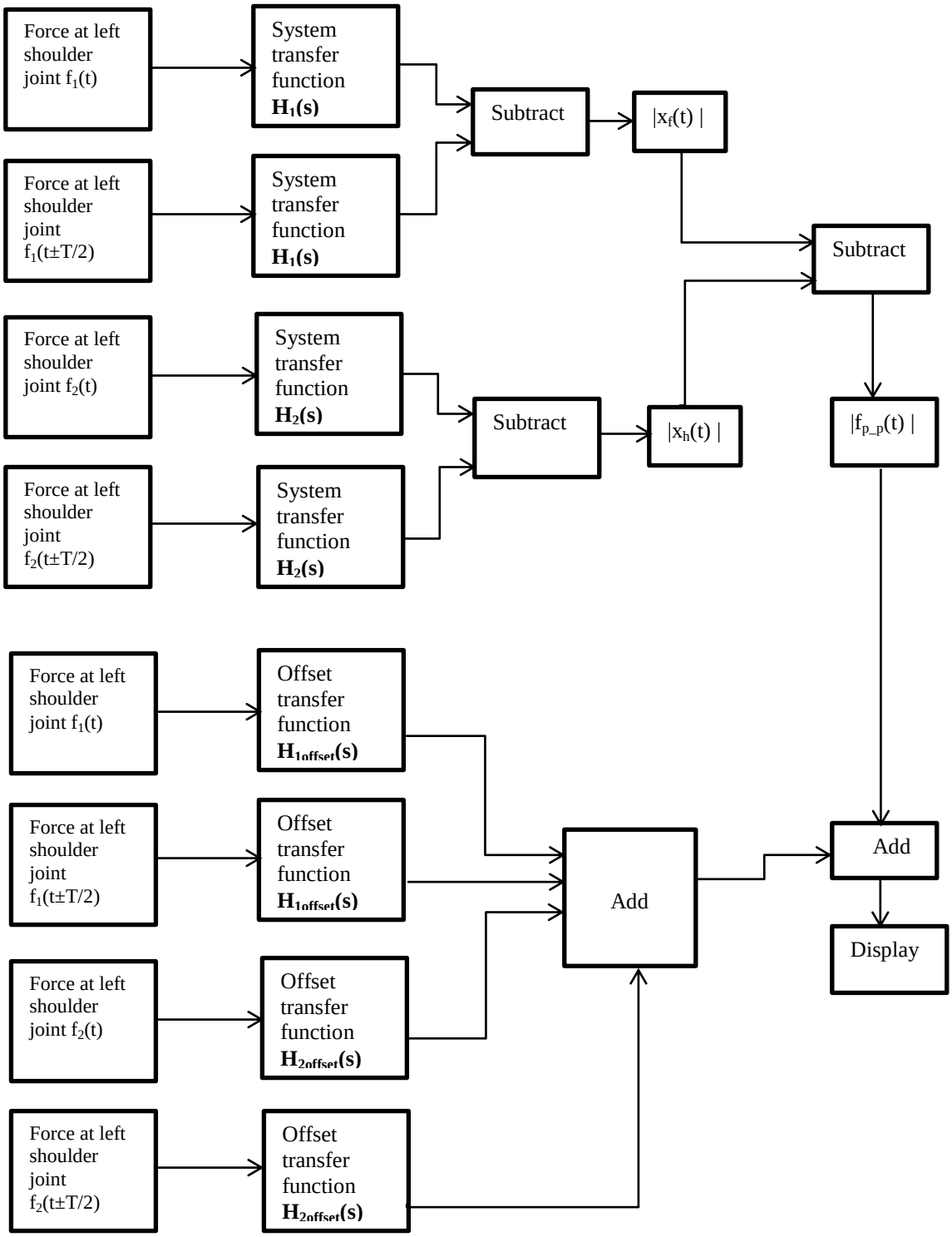

Figure 15: Block diagram of the Simulink (2010a) model to compute the horse back forces using the net joint reaction forces at the shoulder and hip joints.

6. Results

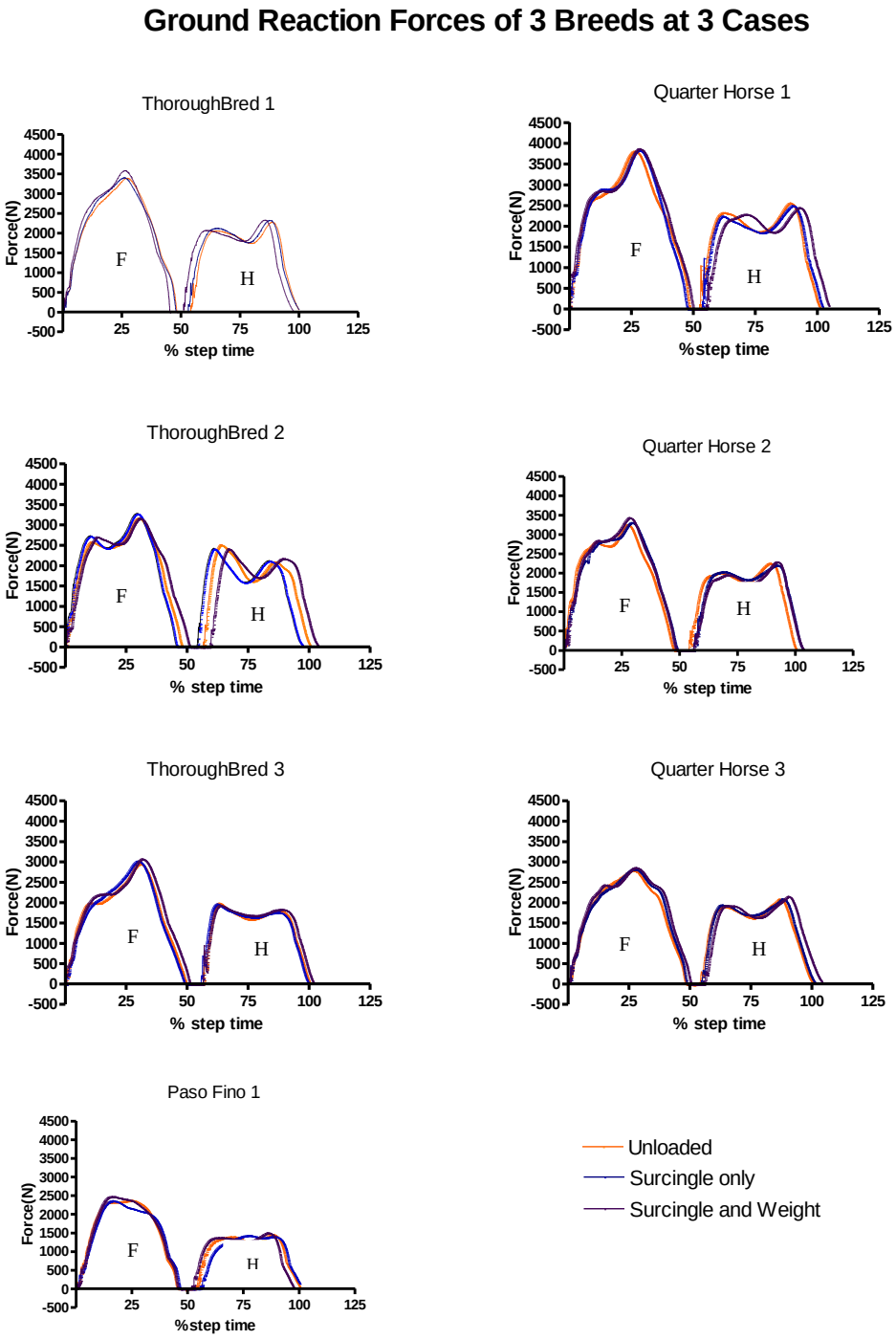

Figure 16: Vertical ground reaction forces (GRFs) of left fore and hind limbs of thoroughbreds, quarter horses and paso fino (Unloaded, with surcingle only and with weight at the back). F- Fore, H- Hind.

Vertical GRFs of all seven horses at the walk for three different conditions are shown in Figure 16. There is no change in GRF pattern or amplitude among three conditions. While no influence on GRF was observed in the situations with surcingle only and surcingle with weight, the net joint forces and are unaffected. These results prove that the GRFs are unchanged with a load that is less than 3% of the horse's weight applied at the horse's back. Consequently, the biomechanical and mathematical model coefficients of the horse are unaffected in this study.

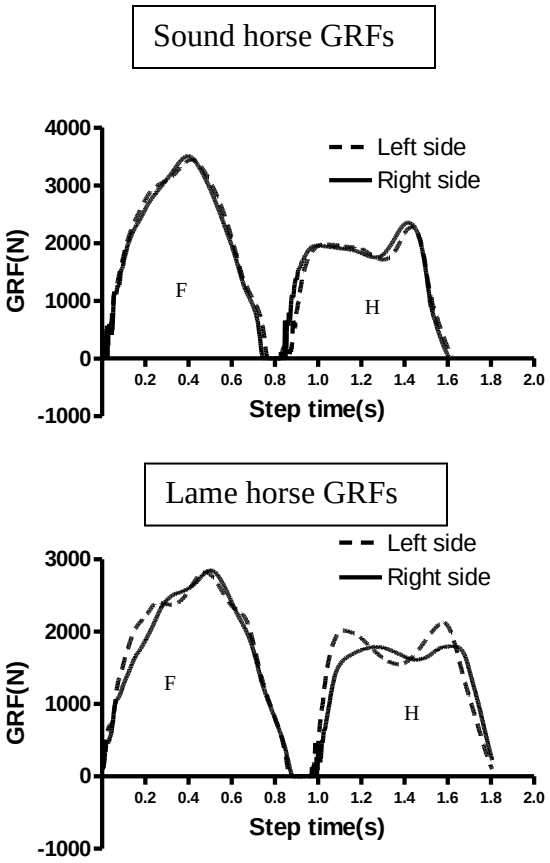

Figure 17: Left and right fore-hind individual limb GRFs of sound and lame thoroughbred over time (not stride cycle). F- Fore, H- hind.

It has been shown that GRFs do not vary significantly from side to side in sound horses. The same does not apply for lame horses, however, as can be seen in Figure 17. Thoroughbred horses have the longest stride time followed by quarter horses and paso fino, respectively (Figure 18).

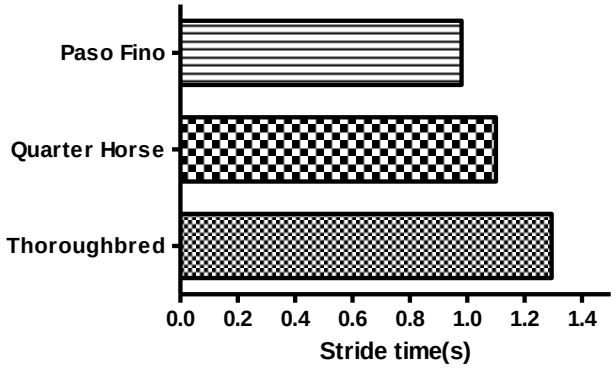

Figure 18: Stride times of one horse per breed, at 1.5±0.1m/s.

Horse 1 Horse 2 Horse 3

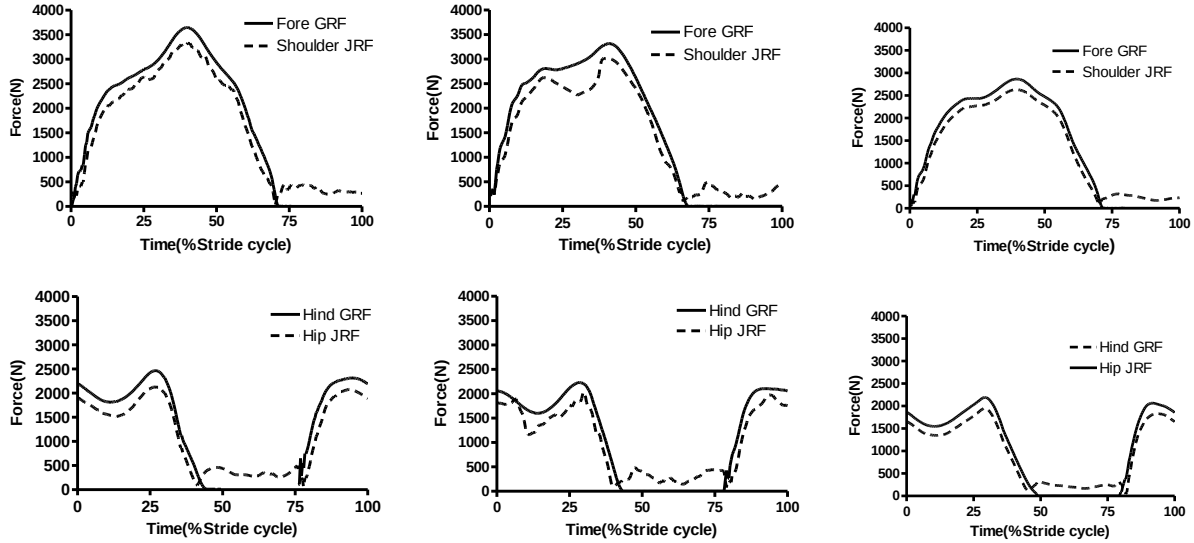

Figure 19: Left side vertical GRFs and net joint reaction forces at the shoulder and hip joint of three thoroughbreds over a stride cycle.

The left fore and hind limb GRFs and net joint reaction forces (JRF) at the left shoulder and left hip joint of thoroughbreds, quarter horses and paso fino are shown Figure 19, 20 and 21, for a single stride. There is a minimal variation in the pattern of GRFs for each individual horse. Peak GRFs of fore- and hind limbs of two sound thoroughbreds are 6.3±0.1N/kg and 4.2±0.07N/kg, respectively. Peak GRFs of fore- and hind limbs of three sound quarter horses are 6.5±0.3N/kg and 4.2±0.2N/kg, respectively. Peak GRFs of fore- and hind limbs of paso fino are

7.1N/kg and 4.3N/kg, respectively. Peak GRFs of fore- and hind limbs of lame thoroughbred are 6.6N/kg and 5.0N/kg, respectively. Paso fino has higher GRF than quarter horses followed by thoroughbreds. TB H3 load left limbs more due to lame on right.

Net joint reaction forces are the equal and opposite forces that exist between adjacent bones at those joints caused by the weight and inertial forces of lower segments. The net joint reaction forces at the shoulder and hip joint are the transferred GRFs from the ground through the lower limb segments. The magnitude of the forces at both the shoulder and hip joints was proportional to the weight of the horse at similar velocity and accelerations. The net joint reaction forces at the hip and shoulder joint have a similar pattern of vertical GRFs with reduced amplitude during the stance phase. Peak JRFs of fore- and hind limbs of the two sound thoroughbreds with weight 555.5±28.9kg are 3171.5±215.5N and 2080.6±63.3N, respectively. Peak JRFs of fore- and hind limbs of three quarter horses with weight 502.4±44.4kg are 3031.6±267N and 1863.6±265.6N, respectively. Peak JRFs of fore- and hind limbs of paso fino with weight 368kg are 2440N and 1351N, respectively. Peak JRFs of fore- and hind limbs of the lame thoroughbred (weight 431kg) are 2632N and 1947N, respectively. The net JRFs at the shoulder joint of thoroughbreds, quarter horses and paso fino are 91.3±0.3%, 92.3±0.2% and 93.4±0.3% of forelimb GRFs, and the net JRFs at the hip joint are 86.5±0.7%, 89±0.8% and 91% of hind limb GRFs during each stance, respectively. The peak net JRFs during the stance phase are proportional to the weight of the horse. Higher amount of GRFs are transferred through the limbs in paso fino followed by quarter horses and thoroughbreds. Left and right fore- and hind limb net JRFs of one of the experimental horses over a stride cycle are shown in Figure 22. The JRFs from both left and right shoulder and hip joints are applied to the spring-damper system to obtain the horse back forces.

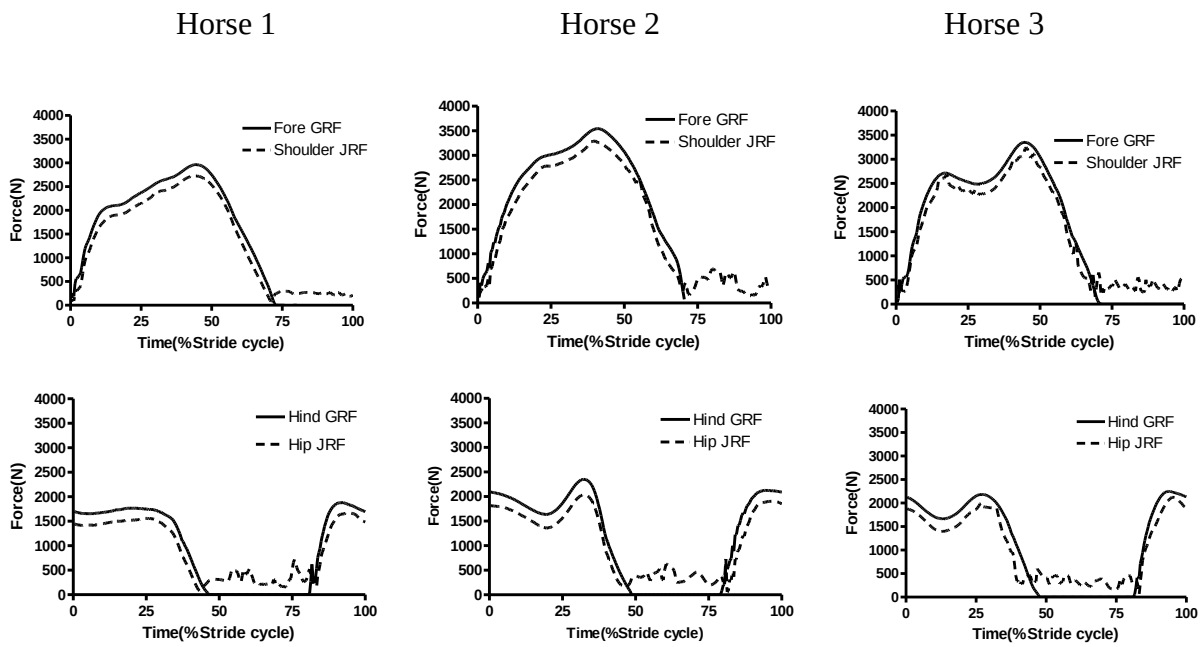

Figure 20: Left side vertical GRFs and net joint reaction forces at the shoulder and hip joint of three quarter horses over a stride cycle.

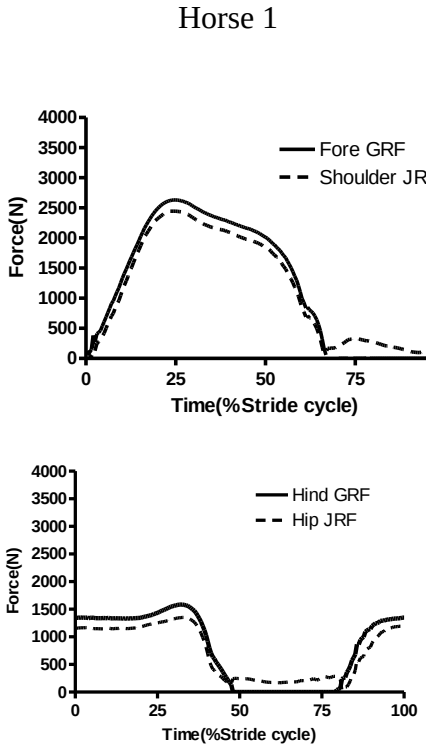

Figure 21: Left side vertical GRFs and net joint reaction forces at the shoulder and hip joint of a paso fino over a stride cycle.

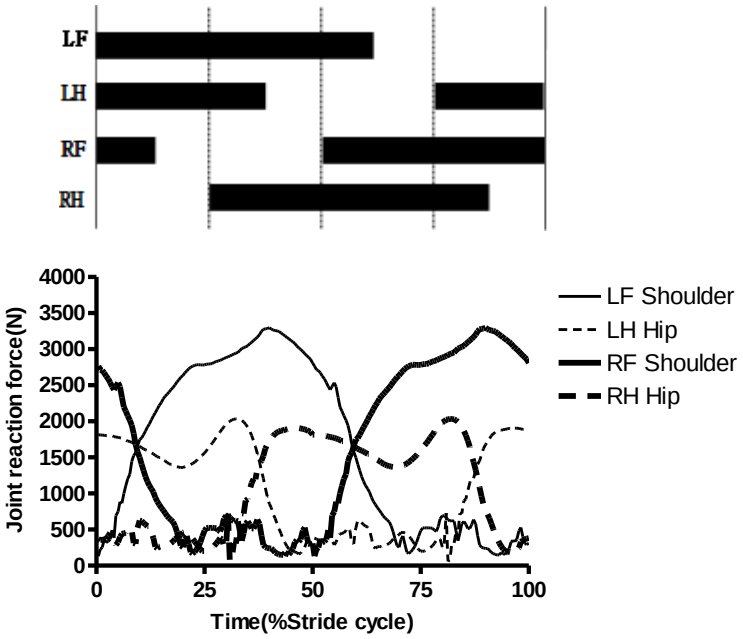

Figure 22: Net joint reaction forces at the shoulder and hip joints of all the limbs over a stride cycle of a sample horse

Measured horse back forces beneath a 12 kg weight are shown in Figure 23, 24 and 25 for three breeds of horses. For all the horses, first peak value occurs within the 25- 50% of the stride cycle. Though the overall pattern of the force is similar for all the horses, there is significant variation in peak and low values from breed to breed and horse to horse. And also, these forces are multifactorial variable depending on age and breed. Two Thoroughbred horses of the same age showed similar force patterns. Peak forces from the 12kg weight on the horse back are 136.5±1.1N, 143.6±3.1N and 153.5N for thoroughbreds, quarter horses and paso fino, respectively (Table 2). Paso fino produces 12.5% and 7% greater peak horse back force than thoroughbreds and quarter horses, respectively according to the measured forces. Whereas, quarter horses produces 5.2% more peak horse back forces than thoroughbreds. The force at horse's back is based on the breed of the horse and it doesn't show any significant variation with the weight of the horse (Table 2).

Table 2: Measured peak forces from 12kg weight on the horse back for three thoroughbreds, three quarter horses and one paso fino.

	Thoroughbred (TB)	**QuarterHorse (QH)**	**Paso Fino (Paso)**
	Peak force from 12kg weight on the horse back (N)	*Peak force from 12kg weight on the horse back (N)*	*Peak force from 12kg weight on the horse back (N)*
H1	**135**	**140**	**153.5**
H2	**137.3**	**143.3**	**N/A**
H3	**137.1**	**147.5**	**N/A**

As mentioned in the methods, the algorithm was programmed in the MATLAB (2010a). The biomechanical model of the horse up to the level of shoulder and hip joint was programmed in scripting environment, whereas the mathematical model was executed in a graphical platform (Simulink). The sample outputs of the scripting program are net joint reaction forces at each joint of the limbs (Figure 26). The computed net JRFs at the shoulder and hip for all the seven horses are shown in above Figure 19, 20 and 21. Left shoulder and hip as well as right shoulder and hip net JRFs are fed to the graphical program at appropriate spring and damper coefficients (Ks, Bs, K_h and Bh) for each horse to get the horse back forces comparable to force sensor measured values. The simulated and measured test results can be found in Figure 23, 24 and 25. A significant correlation ($p<0.001$) is observed between measured and simulated values. The correlation coefficients are as follow: Thoroughbreds: 0.81, 0.80 and 0.77, Quarter Horses: 0.84, 0.86, and 0.82, and Paso Fino: 0.75 for the given K and B values. Thoroughbred Horse3 showed significant correlation between simulated results and measured data. Visually however, a stark contrast can be easily discerned. This is due to the fact that Horse3 was found to be slightly lame, and this would lead to asymmetry in the legs which would throw off the simulated data. Here, the K_{s1} and K_{h1} values plays the role in determining the pattern and peak-to-trough output force

of the system, whereas K_{s2} and K_{h2} decides the offset values of the output force. B_{s1}, B_{s2}, B_{h1} and B_{h2} are important in determining the control of oscillations of the system and output patterns of the graphs.

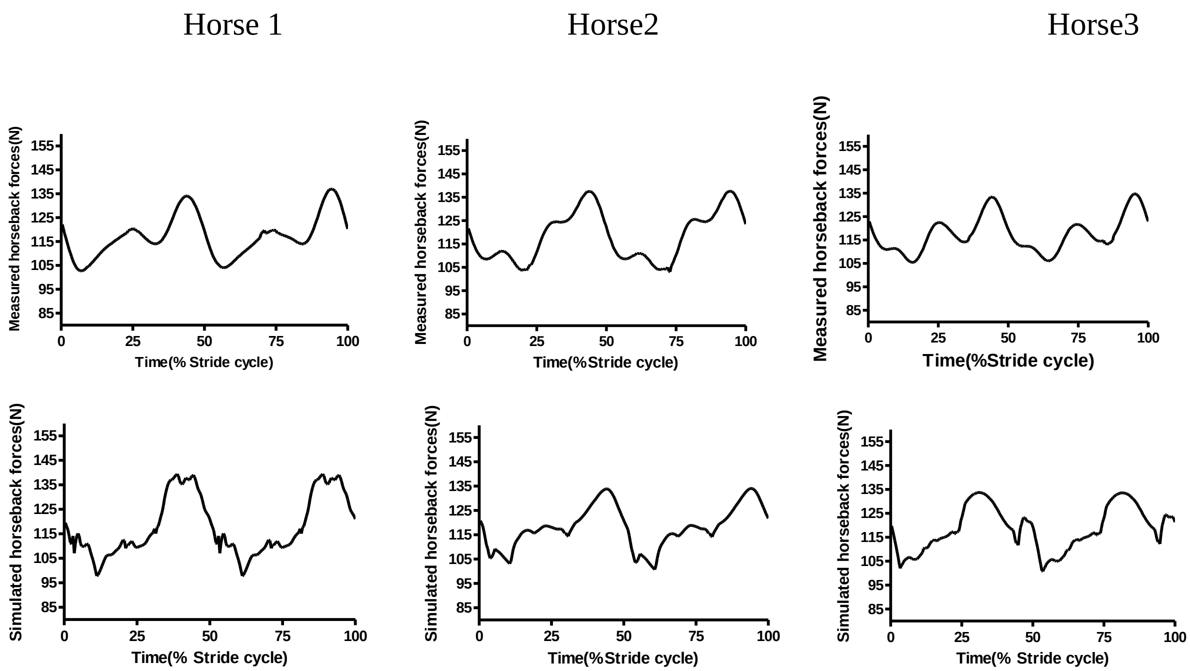

Figure 23: Measured and simulated forces under 12kg weigh on horse back for thoroughbreds

Table 3: Spring and damper coefficients of the mathematical model for individual horses of thoroughbred, quarter horse, and paso fino(mean±sd).

	Thoroughbred (TB)				**Quarter Horse (QH)**				**Paso Fino(Paso)**			
	K_{s1}, K_{s2} (N/m)	*B_{s1}, B_{s2} (Ns/m)*	*K_{h1}, K_{h2} (N/m)*	*B_{h1}, B_{h2} (Ns/m)*	*K_{s1}, K_{s2} (N/m)*	*B_{s1}, B_{s2} (Ns/m)*	*K_{h1}, K_{h2} (N/m)*	*B_{h1}, B_{h2} (Ns/m)*	*K_{s1}, K_{s2} (N/m)*	*B_{s1}, B_{s2} (Ns/m)*	*K_{h1}, K_{h2} (N/m)*	*B_{h1}, B_{h2} (Ns/m)*
H1	131±3.4, 34±2.8	0.8±0.5, 0.9±0.4	225±10.6 225±10.6	5.3±4.8, 8.2±2.1,	61.5±2.1, 31±2.3	1.8±0.6 0.9±0.3	138±6.8 138±6.8	6.2±4.3, 6.2±4.3,	51.5±2.1 21.5±2.4	1.5±0.8 1.3±0.9	160±6.2 160±6.2	6.2±3.7. 6.2±3.7
H2	122±2.7, 32±2.8	2.5±1.3, 1.8±0.8	204±8.2, 204±8.2	10.2±3.5, 7.5±2.4	92.5±3.5, 31.5±3.4	0.8±0.5, 1.2±0.2	162±8.4 162±8.4	7.2±3.5, 7.2±3.5	-	-	-	-
H3	71±2.7, 34±1.5	1.8±0.8, 1.8±0.9	184±7.0, 184±7.0	7.3±3.2, 6.1±2.2	68±3.1, 73±3.8	1.5±0.7, 2.4±0.6	168±7.3 168±7.3	4.5±3.8, 9.4±3.8	-	-	-	-

Fore- and hind limb side spring coefficients of two sound thoroughbreds with weight 555.5±28.9kg are 126.5±6.3N/m and 214.5±14.8N/m, respectively. Fore- and hind limb side

spring coefficients of three quarter horses with weight 502.4±44.4kg are 74±16.3N/m and 156.3±15.8N/m, respectively. Fore- and hind limb side spring coefficients of paso fino with weight 368 kg are 51.5±2.1N/m and 150N/m, respectively. Fore- and hind limb side spring coefficients of lame thoroughbred with weight 431kg are 71±2.5N/m and 184±7.0N/m, respectively. Thoroughbreds have higher shoulder spring coefficients compared with quarter horses and paso fino. These coefficient values increase with the weight of the horse within the breed. The damper coefficients for all the horses vary based on the pattern of the horse back force which is a multifactorial variable. These values help in changing the oscillations of the system which can affect the horse back force patterns.

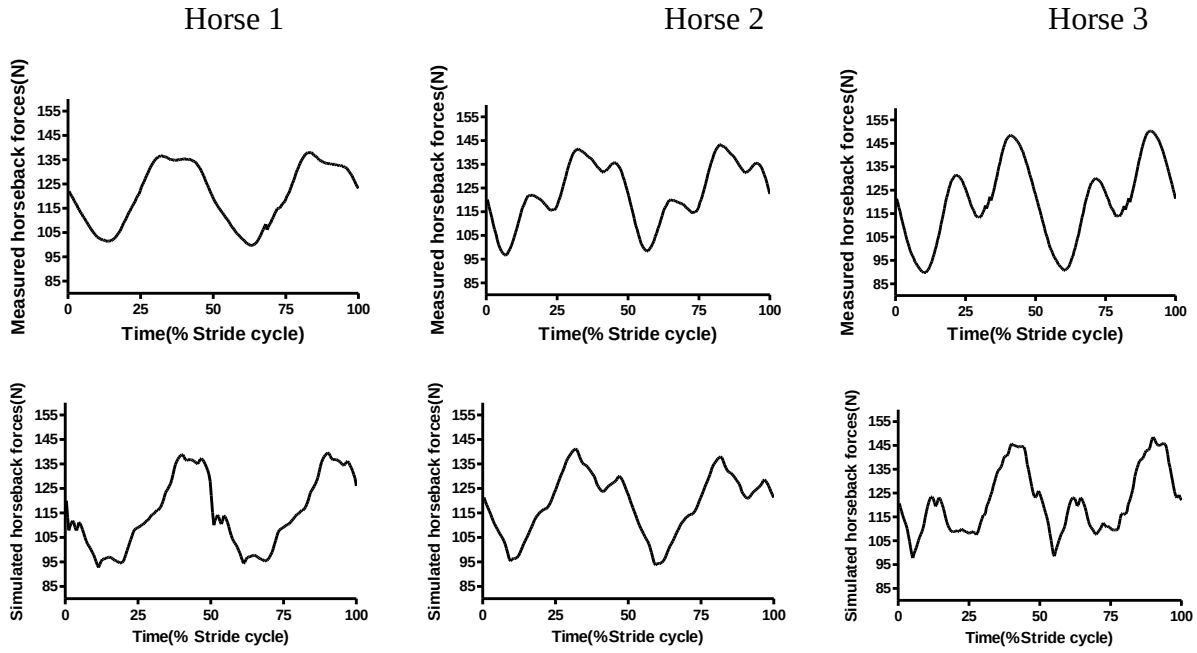

Figure 24: Measured and simulated forces under 12kg weigh on horse back of quarter horses

Horse 1

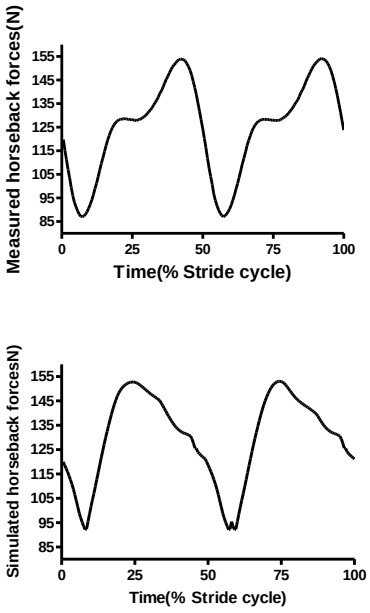

Figure 25: Measured and simulated forces under 12kg weigh on horse back of paso fino

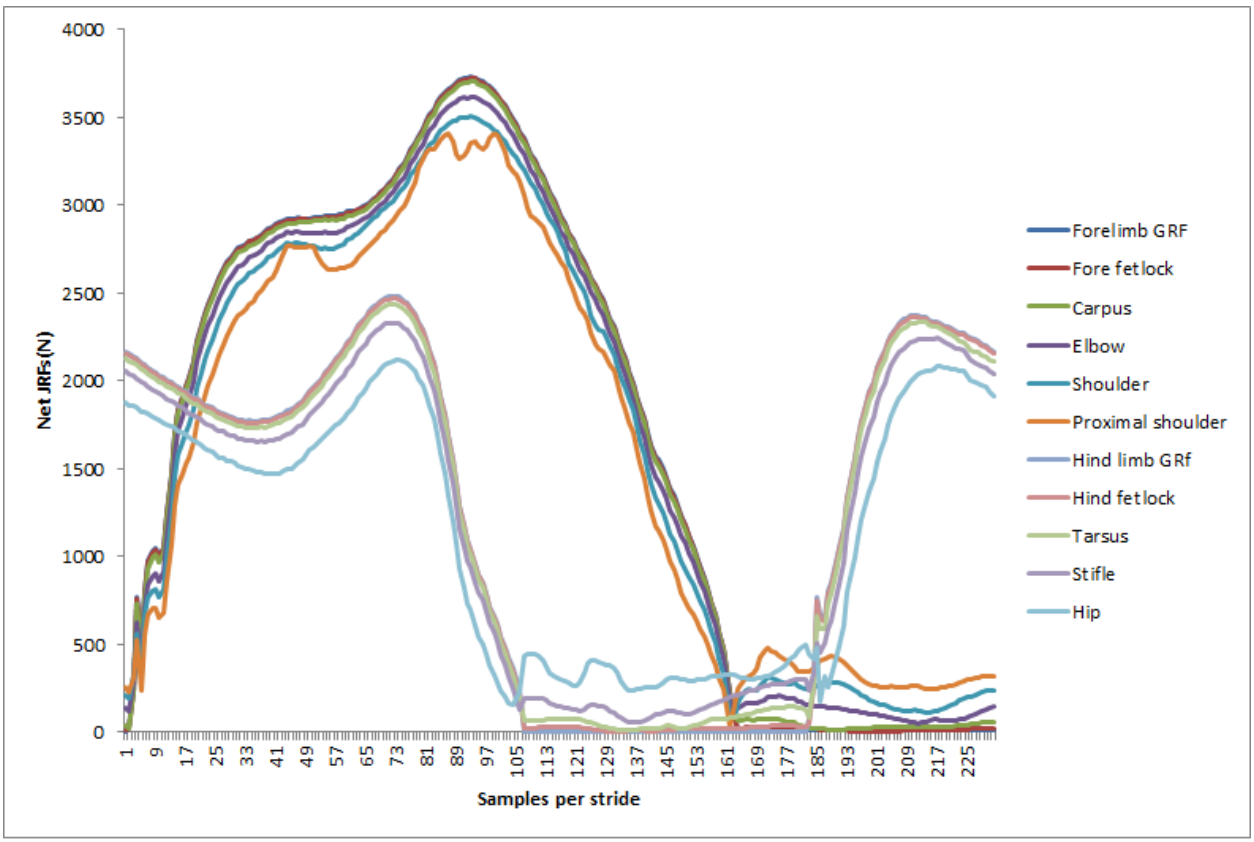

Figure 26: Simulated net joint reaction forces using MATLAB program for thoroughbred H1

- **Approximate Model**

It is observed that the net joint reaction forces follow the similar pattern of GRFs with reduced amplitude in stance and raised amplitude in swing. It is a thought applied to test the horse back spring-damper model with GRFs. The GRFs from all four limbs fed to the spring-damper model instead of net JRFs from shoulder and hip joints. The horse back forces from this approximate model for all the horses are shown in Figure 27. It is observed that the approximate model forces follow the approximately similar patterns of accurate model forces with shifted amplitude. This model can be used in the applications that do not need accurate patterns and amplitudes.

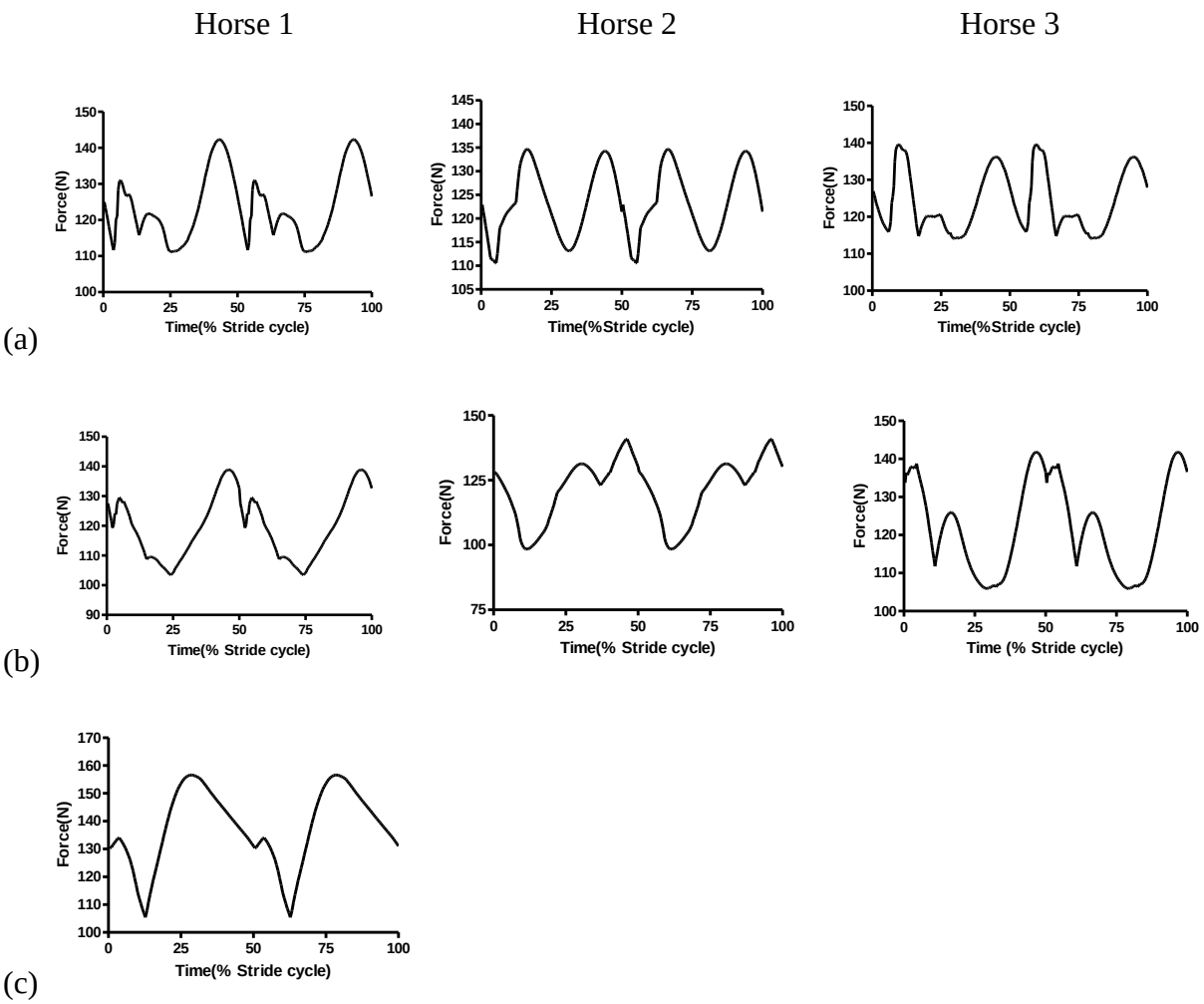

Figure 27: simulated horse back forces with the approximate model. a) Thoroughbreds; b) Quarter horses; c) Paso fino.

7. Discussion and Conclusion

Therapeutic horseback riding is an effective form of physical and emotional therapy that has been widely used for centuries. Since the effectiveness of the therapy is dependent on what the rider experiences, appropriate horse-rider matching is necessary for successful therapy (Hammer, Nilsagård et al. 2005; Lessick, Shinaver et al. 2006). Body models and computer simulations are viable methods to study the mechanical aspects of systems and are widely used to develop better safety procedures and strategies (Crispino, Tasora et al. 2005). Quantification of the forces at horse's back is valuable for therapists as the analysis of these forces yields better therapy quality and an overall better experience for the rider. This study focused on developing a computer model to simulate the horse back forces using horse GRFs and kinematics. To the author's knowledge, this type of analysis of the horse back forces has not been attempted before, and the model is the first to offer an explanation of the relationship between the horse motion and the horse back forces. The model can expedite the process of matching a horse to a rider, since the specific rider needs yield a certain horse size, weight, and gait pattern. The simulation model serves as a solid foundation for the development of a horse database for therapeutic riding.

The horse is a complex biomechanical machine. This study focused on reducing the equine limbs and back into a simple model that would represent the underlying biomechanical principles of horse locomotion. In order to do this, two separate models were integrated together to form a system. The limbs are represented with an open-chain link model while the back is modeled with two sets of springs and dampers (Clayton, Hodson et al. 2000; Hodson, Clayton et al. 2001; Peham and Schobesberger 2004). 2-D conventional inverse dynamic analysis was performed on kinematic and kinetic data from seven horses in order to determine the physical coefficients for the model of horse locomotion at the walk. Inverse dynamics was used over forward dynamics to

simplify the mathematical complexity. Since forward dynamics calculates the motion of the body based on given forces and moments. But human motion can be captured non-invasively than the forces and torques. Thus the inverse dynamics can reduce the complexity of the model. The mathematical model developed describes the back of the horse as a series of springs and dampers in order to more accurately represent the physical action of the muscles and spine in this area. These two systems together allow for a comprehensive analysis of the relationship between the GRFs and horse back forces. This simple model structure reflects essential aspects of the biomechanics of the limb segments and equine back and also it is mathematically tractable. One should not mistake the model for an anatomically realistic simulation of the equine back. This model is not anatomically accurate, but solely mimics the biomechanical behavior of the limbs and equine back.

Seven horses were used in this study, specifically three thoroughbreds, three quarter horses, and one paso fino. The size of the sample does not have the statistical power to generate a complete database as reference for the mechanical coefficients of the system based on horse weight, size, and age. However, it is possible to predict the effects of weight on the coefficients. Different breeds differed in the mechanical coefficients required for a successful simulation. Weight increased the spring coefficients, and thoroughbreds required the highest values compared to the other horses. The use of k and b values is implemented to simulate the barrel of the horse. The specific relationship between k and b values and horse breed and gait cannot be determined from this study alone. Further analysis of the movement characteristics is necessary to establish a concrete relationship between suitable k and b values and horse gait and physiology. This idea relates to the fact that the paso fino horse presented the highest horse back forces. It is well known that paso finos are horses with a steady and stabilized gait that does not

affect the rider (paso fino is Spanish for ‘fine gait’), which points to the conclusion that the specific movements of the gait of a paso fino distribute forces through the horse back away from the rider, instead of terminating at the back. There is only one sample paso fino horse, which limits the confidence that can be had when drawing conclusions based on horse breed.

Other studies demonstrated that GRFs changed with the weight of the horse and the load on the horse back (Clayton, Lanovaz et al. 1999). The results of this study showed no appreciable change in GRFs with the applied load. This is due to the relative small size of the mass of the load when compared to the mass of the horse. The results show that the relationship between weight and the spring constant (k) is proportional, with the mean coefficient value determined by the breed.

The inertial properties of the horses used in this study were estimated from recorded values for Dutch warmblood horses (Buchner, Savelberg et al. 1997). The method to use the inertial properties of Dutch warmblood is described in this study, but to the author’s knowledge, this is the first time the pertinent model to compute the inertial properties from given data of a reference horse is described in detail. It was assumed that the mass, length, and size of the horses used were directly proportional to the reference horse.

It was also assumed that the gait of the horses studied is symmetrical, as shown in previous studies involving gait analysis (Pourcelot, Audigie et al. 1997). The data was obtained in a sequential fore to hind cycle; however, detailed analysis of the horse walk reveals that there are three limbs on the ground at any point in time. The fore and hind limbs for the same side are on the ground for a specified period of the stride cycle. The measured fore to hind cycle was calculated according to the horse gait cycle to obtain the real GRF results as the GRFs are consistent over many strides.

The procedure used to analyze equine motion is similar to the current procedures established to analyze human gaits. It compares to the high-order human analysis as described by J. K. Aggarwal (Aggarwal and Cai 1997). It differs, however, by the fact that human motion analysis involves studying a biped with alternating steps, while the horse gait involves a more complex quadruped gait with 2 and 3 beat alternations at the walk, and more complicated motion at the trot and canter. It also differs anatomically as the horse body cannot be modeled with rigid chain-links, since the shoulder of the horse is not connected to the forelimbs with a bone joint.

Joint reaction forces are important for prevention of equine injury (Merritt, Davies et al. 2007). This model solves for JRFs at nine joints from the hoof to the back using GRFs. It is noteworthy that the calculated JRFs in this case are similar in magnitude to the GRF minus the weight of the limbs, especially when the magnitude of the limb acceleration is small. Information related to JRFs can be used to implement more effective protocols for injury prevention. Computer simulation models of various transportation vehicles like bicycles and motorcycles are used to improve the safety of the rider (Crispino, Tasora et al. 2005). Similarly, specific athletic requirements and protective gear for both the horse and the rider can be customized using this model (Von Peinen, Wiestner et al. 2010). Since this model is proven to work with different breeds of horses, it is expected that its advantages will not be limited by the user's lack of experience with or the availability of other breeds.

The biomechanical model proved to be satisfactorily accurate in simulating horse back forces. The correlation test results between measured and the simulated output showed a minimum of 75% and a maximum of 86.3%, with the minimum correlation being related to the lame horse. The correlation test results show that the model is rigorous enough to account for a limited amount of variability due to injury or small differences in the horse gait.

C. Peham (Peham and Schobesberger 2004) performed a study using a force sensor mat to measure the pressure forces from the rider onto the horse back. This method had the limitation that the force component from the horse or the rider cannot be determined. Instead, the net action-reaction forces are calculated which occur on the horse back. This model goes a step beyond and allows for the calculation of the horse back forces coming from the horse. Future work could involve the application of a force sensing mat to determine the force component from the horse and rider, and lead to greater insight of the effect of the rider on the horse. The measured vertical horse back forces at the walk are also similar to results presented by C. Peham (Peham and Schobesberger 2004). Variation between the results cannot be explained because horse breed is not defined in the study by C. Peham (Peham and Schobesberger 2004).

To the author's knowledge, there is no study that explains the relationship between the GRFs and the forces at horse's back. (Clayton, Hodson et al. 2000; Hodson, Clayton et al. 2001) used inverse dynamics to calculate the JRFs from GRFs; this study however, focuses on calculating the horse back forces. These forces are coupled with a physical model that implements springs and dampers to estimate the forces experienced by a load. C. Peham (Peham and Schobesberger 2004) developed a biomechanical model of the equine spine using interconnected cylindrical segments and the long back muscles using springs. This study also uses springs to represent the muscular equine back, and couples this system with an open-chain link model for the horse's limbs. The model system was used to simulate equine locomotion and help explain the relationship between the GRFs and the forces experienced at the saddle.

This biomechanical model can be simplified using impulse response functions. It was found that the impulse response functions were exponential in nature. The characteristic impulse response function of the simulation is useful for the widespread application and flexibility of the

model, while it enables the end-user to obtain results with a small amount of data processing. This is important for future program design and optimization, and allows for different approaches to be considered when designing data collection protocols for GRFs.

The methods implemented in this study are novel to the study of equine motion analysis and future studies can gain from and improve on the proposed methods. This model can also be implemented in future studies that attempt to model equine motion with a saddle rider. This same method can also be used as a baseline

in the study of motion and forces of other quadruped animals and machines. The motion capture data and joint forces can also be applied in computer animation to develop more accurate animated models (James and Twigg 2005).

This study focused on locomotion horse data at the walk. The mathematical model was developed to utilize 2-dimensional data to simulate the horse walk. A database was developed that pursued 3-D inverse dynamic analysis, but this aspect of the study had to be dropped because of the fact that the Codamotion software does not currently support the necessary kinematic data output to be used in a segmental coordinate system for the application of the inverse dynamic analysis. In addition, the Codamotion manual and website do not clearly explain the technology behind the sensors to support the specified resolution values, and due to lack of time the resolution specifications of the system could not be corroborated experimentally. The study was also limited to the analysis of a single equine gait, namely the walk. This is limited from the three distinguishable gaits, the others being the trot and the canter. It was not possible to work with many different horse breeds and further study is needed on this matter. Additionally, the study was performed with a static weight on the back of the horse. Future work should consider the functional dynamic forces from the rider on this system.

In summary, the goal of this study was simulating the horse back forces of various breeds. A biomechanical model in conjunction with mechanical components was developed to solve the system equations with various coefficients. This model will set a solid foundation for the development of a horse database that will aid therapeutic riding in the process of horse and rider pairing. The model however, is not anatomically faithful, but rather a biomechanical simplification of the horse limbs and back. The spring and damper coefficients implemented in the model are determined by the physiology of the horse, but further study is required to establish the relationship between horse characteristic gait, physiology, and coefficients. It is possible to say, however, that spring coefficients are proportional to horse weight within breeds.

References

Aggarwal, J. K. and Q. Cai (1997). Human motion analysis: A review, IEEE.

All, A., G. Loving, et al. (1999). "Animals, Horseback Riding, and Implications for Rehabilitation Therapy." J Rehabil **65**(3).

Apkarian, J., S. Naumann, et al. (1989). "A three-dimensional kinematic and dynamic model of the lower limb." J Biomech **22**(2): 143-155.

Back, W., C. MacAllister, et al. (2007). "Vertical frontlimb ground reaction forces of sound and lame Warmbloods differ from those in Quarter Horses." J Equine Vet Sci **27**(3): 123-129.

Bertoti, D. B. (1988). "Effect of Therapeutic Horseback Riding on Posture in Children with Cerebral Palsy." Phys Ther **68**(10): 1505-1512.

Biknevicius, A., D. Mullineaux, et al. (2004). "Ground reaction forces and limb function in tölting Icelandic horses." Equine Vet J **36**(8): 743-747.

Bliss, B. (1997). "Complementary therapies--therapeutic horseback riding?" RN **60**(10): 69.

Buchner, H. H., H. H. Savelberg, et al. (1997). "Inertial properties of Dutch Warmblood horses." J Biomech **30**(6): 653-658.

Chandler, R., C. Clauser, et al. (1975). Investigation of inertial properties of the human body, NTIS, National Technical Information Service.

Clayton, H., E. Hodson, et al. (2000). "The forelimb in walking horses: 2. Net joint moments and joint powers." Equine Vet J **32**(4): 295-300.

Clayton, H., E. Hodson, et al. (2001). "The hindlimb in walking horses: 2. Net joint moments and joint powers." Equine Vet J **33**(1): 44-48.

Clayton, H. M., J. Lanovaz, et al. (1999). "The effects of a rider's mass on ground reaction forces and fetlock kinematics at the trot." Equine Vet J **31**(S30): 218-221.

Clayton, H. M., H. C. Schamhardt, et al. (2000). "Kinematics and ground reaction forces in horses with superficial digital flexor tendinitis." Am J Vet Res **61**(2): 191-196.

Cocq, P., P. Weeren, et al. (2004). "Effects of girth, saddle and weight on movements of the horse." Equine Vet J **36**(8): 758-763.

Codamotion. "Codamotion products." from http://www.codamotion.com/engineering-systems-overview.html.

Colborne, G., J. Lanovaz, et al. (1997). "Joint moments and power in equine gait: a preliminary study." Equine Vet J Suppl(23): 33.

Crispino, M., A. Tasora, et al. (2005). "New method to assess ride safety on uneven element pavements." J Transp Eng **131**: 27.

Crowe, A. (1968). "A Mechanical Model of Mammalian Muscle Spindle." J Theor Biol **21**(1): 21-&.

De Jalon, J. and E. Bayo (1994). Kinematic and dynamic simulation of multibody systems, Springer New York.

Doriot, N. and L. Cheze (2004). "A three-dimensional kinematic and dynamic study of the lower limb during the stance phase of gait using an homogeneous matrix approach." IEEE Trans Biomed Eng **51**(1): 21-27.

Dumas, R., R. Aissaoui, et al. (2004). "A 3D generic inverse dynamic method using wrench notation and quaternion algebra." Comput Methods Biomech Biomed Engin **7**(3): 159-166.

Dumas, R., E. Nicol, et al. (2005). "Comparison of four 3D inverse dynamic methods for gait analysis." Comput Methods Biomech Biomed Engin **8**: 89-90.

Erdemir, A., S. McLean, et al. (2007). "Model-based estimation of muscle forces exerted during movements." Clin Biomech **22**(2): 131-154.

Faber, M., H. Schamhardt, et al. (2001). "Methodology and validity of assessing kinematics of the thoracolumbar vertebral column in horses on the basis of skin-fixated markers." Am J Vet Res **62**(3): 301-306.

Faber, M., H. Schamhardt, et al. (2000). "Basic three-dimensional kinematics of the vertebral column of horses walking on a treadmill." Am J Vet Res **61**(4): 399-406.

Glitsch, U. and W. Baumann (1997). "The three-dimensional determination of internal loads in the lower extremity." J Biomech **30**(11): 1123-1131.

Hammer, A., Y. Nilsagård, et al. (2005). "Evaluation of therapeutic riding (Sweden)/hippotherapy (United States). A single-subject experimental design study replicated in eleven patients with multiple sclerosis." Physiother Theory Pract **21**(1): 51-77.

Hinrichs, R. N. (1985). "Regression analysis to predict segmental moments of inertia from anthropomorphic measurements: an extension of the data of Chandler et al. (1975)." J Biomech **18**: 621-624.

Hodson, E., H. Clayton, et al. (2001). "The hindlimb in walking horses: 1. Kinematics and ground reaction forces." Equine Vet J **33**(1): 38-43.

Hodson, E., H. Clayton, et al. (2010). "The forelimb in walking horses: 1. Kinematics and ground reaction forces." Equine Vet J **32**(4): 287-294.

James, D. L. and C. D. Twigg (2005). Skinning mesh animations, ACM.

Janice, J. E. and A. W. David (1995). "Kinetic analysis of the lower limbs during walking: What information can be gained from a three-dimensional model?" J Biomech **28**(6): 753-758.

Lagarde, J., C. Peham, et al. (2005). "Coordination dynamics of the horse-rider system." J Mot Behav **37**(6): 418-424.

Lee, K. P., T. W. Koo, et al. (1998). Real-time dynamic simulation of quadruped using modified velocity transformation, IEEE.

Legnani, G., F. Casolo, et al. (1996). "A homogeneous matrix approach to 3D kinematics and dynamics--I. Theory." Mech Mach theory **31**(5): 573-587.

Lehrman, J. and D. B. Ross (2001). "Therapeutic Riding for a Student with Multiple Disabilities and Visual Impairment: A Case Study." J Vis Impair Blind **95**(2): 108-109.

Lessick, M., R. Shinaver, et al. (2006). "Therapeutic Horseback Riding." AWHONN Lifelines **8**(1): 46-53.

MacKinnon, J. R., S. Noh, et al. (1995). "A study of therapeutic effects of horseback riding for children with cerebral palsy." Phys Occup Ther Pediatr **15**(1): 17-34.

MacPhail, H., J. Edwards, et al. (1998). "Trunk postural reactions in children with and without cerebral palsy during therapeutic horseback riding." Pediatr Phys Ther **10**(4): 143.

Martin, C. and L. Schovanec (1998). "Muscle mechanics and dynamics of ocular motion." Journal of Mathematical Systems Estimation and Control **8**: 233-236.

Merkens, H., H. Schamhardt, et al. (1986). "Ground reaction force patterns of Dutch Warmblood horses at normal walk." Equine Vet J **18**(3): 207-214.

Merritt, J. S., H. M. S. Davies, et al. (2007). Calculation of Joint Reaction Forces in the Equine Distal Forelimb during Walking and Trotting, IEEE.

motion, A. f. a. "BP900900 force platform." from http://www.forceandmotion.com/select%20product%20PDFs/Biomechanics%20force%20platforms/BP900900%20brochure.pdf.

Peham, C. and H. Schobesberger (2004). "Influence of the load of a rider or of a region with increased stiffness on the equine back: a modelling study." Equine Vet J **36**(8): 703-705.

Phillips, C. and V. Aspinall (2006). "Equine anatomy and physiology." The complete textbook of veterinary nursing: 133-144.

Pourcelot, P., F. Audigie, et al. (1997). "Kinematic symmetry index: a method for quantifying the horse locomotion symmetry using kinematic data." Vet Res **28**(6): 525.

Silva, M. and J. Ambrósio (2002). "Kinematic data consistency in the inverse dynamic analysis of biomechanical systems." Multibody Syst Dyn **8**(2): 219-239.

Silva, M., J. Ambrosio, et al. (1997). "Biomechanical model with joint resistance for impact simulation." Multibody Syst Dyn **1**(1): 65-84.

Tekscan, I. "ELF system user manual." from http://www.tekscan.com/pdfs/ELFUserManual.pdf.

Tekscan, I. "Flexi force sensors." from http://www.tekscan.com/flexiforce/flexiforce.html.

Tekscan, I. "Wireless ELF system." from http://www.tekscan.com/pdfs/WELF.pdf.

van den Bogert, A. (1989). "Computer simulation of locomotion in the horse." PhD, Utrecht.

van Gurp, M., H. Schamhardt, et al. (1986). "Dynamic model of the equine hindlimb during the swing phase." Cells Tissues Organs **127**(4): 279-284.

Vaughan, e. a. (1992). Dynamics of human gait. Illinois: Champaign.

Von Peinen, K., T. Wiestner, et al. (2010). "Relationship between saddle pressure measurements and clinical signs of saddle soreness at the withers." Equine Vet J **42**: 650-653.

Zhang, L., D. Xu, et al. (2000). Stiffness and viscous damping of the human leg.

Appendix: Computer Program

Computing the CoM axis components of each segment of horse limbs to represent the CoM as virtual markers in Codamotion software

```
% Computing the center of mass and weights for codamotion system of eachsegment
clear all;
clc;
% storing the marker position ratio obtained from dutch warm blood horses of complete 9
segments

ratio = [33,-11,46;17.4,-1.0,44;14.2,-2.1,35;30,-5.0,51;21.0,-12,27;29,-13,43;13.3,-6.7,32;14,-
8.4,37.9;20.6,-12,59]; % reference ratio wrt length of each segment
Num =
xlsread('E:\ThesisRelated\HORSE_MOTION_DATA\Computer_programs\CoM_Computation.x
lsx', 1); % read the excel sheet
[Num_rows, Num_columns] = size(Num); % computes number of rows and columns in the
excel sheet
Num_segments = Num_columns/6; % computes number of segmnets from number of columns
in the sheet
Segment_length = zeros(Num_rows, Num_segments);
x = zeros(Num_rows, 2 * Num_segments);
y = zeros(Num_rows, 2 * Num_segments);
z = zeros(Num_rows, 2 * Num_segments);
CoM_X = zeros(Num_rows, Num_segments);
CoM_Y = zeros(Num_rows, Num_segments);
CoM_Z = zeros(Num_rows, Num_segments);
ProxCoMdist = zeros(Num_rows, Num_segments);
Weight = zeros(Num_rows,Num_segments);
disp(Num_segments);

% storing the x, y, z position of each marker in all segments
for i = 1: Num_rows
    k = 1;
    for j = 1: 2 * Num_segments
      x(i,j) = Num(i,k);
      k = k+1;
      y(i,j) = Num(i,k);
      k = k+1;
      z(i,j) = Num(i,k);
      k = k+1;
    end
end
disp(x);
```

```
% computes the length, Center of Mass and weight for codamotion from the proximal end of
each segment
for i = 1: Num_rows
   for j = 1 : 2 : 2 * Num_segments
      k = 1;
      Segment_length(i,(j+1)/2) = realsqrt((x(i,j)-x(i,j+1))*(x(i,j)-x(i,j+1))+(y(i,j)-
y(i,j+1))*(y(i,j)-y(i,j+1))+(z(i,j)-z(i,j+1))*(z(i,j)-z(i,j+1)));
      CoM_X(i,(j+1)/2) = x(i,j+1)+ ratio((j+1)/2,k)* Segment_length(i, (j+1)/2)* 1/100;
      CoM_Y(i,(j+1)/2) = y(i,j+1)+ ratio((j+1)/2,k+1)* Segment_length(i, (j+1)/2)* 1/100;
      CoM_Z(i,(j+1)/2) = z(i,j+1)- ratio((j+1)/2,k+2)* Segment_length(i, (j+1)/2) * 1/100;
      ProxCoMdist(i,(j+1)/2) = realsqrt((CoM_X(i,(j+1)/2)-x(i,j+1))*(CoM_X(i,(j+1)/2)-
x(i,j+1))+(CoM_Y(i,(j+1)/2)-y(i,j+1))*(CoM_Y(i,(j+1)/2)-y(i,j+1))+(CoM_Z(i,(j+1)/2)-
z(i,j+1))*(CoM_Z(i,(j+1)/2)-z(i,j+1)));
      Weight(i,(j+1)/2) = ProxCoMdist(i,(j+1)/2)/ Segment_length(i,(j+1)/2);
   end
end
%disp(Segment_length);
%disp(ProxCoMdist);
disp(CoM_X);
disp(CoM_Y);
disp(CoM_Z);
disp(Weight);
SUCCESS =
xlswrite('E:\ThesisRelated\HORSE_MOTION_DATA\Computer_programs\CoM_Computation.
xlsx', Weight, 2,'B2');
SUCCESS1 =
xlswrite('E:\ThesisRelated\HORSE_MOTION_DATA\Computer_programs\CoM_Computation.
xlsx', CoM_X, 2,'L2');
SUCCESS2 =
xlswrite('E:\ThesisRelated\HORSE_MOTION_DATA\Computer_programs\CoM_Computation.
xlsx', CoM_Y, 2,'U2');
SUCCESS3 =
xlswrite('E:\ThesisRelated\HORSE_MOTION_DATA\Computer_programs\CoM_Computation.
xlsx', CoM_Z, 2,'AD2');
disp(SUCCESS);
%disp(Num);
%disp(x);
%disp(y);
%disp(z);
```

Computing the joint reaction forces

```
% calculation of Joint forces
clear all;
clc;

% storing the mass ratio obtained from dutch warm blood horses of complete 9 segments
```

```
Horse_mass = input('Enter the weight of the horse:');
Excelsheet_name = input('Enter the file name:', 's');
Number_sheets = input('Enter number of sheets in the file:');
mass_ratio = [0.1357 0.29 1.24 1.59 2.13 0.165 0.528 1.543 3.45];
global Ref_mass;
Ref_mass= [0.73 1.59 6.7 8.6 11.5 0.89 2.84 8.3 18.6];
global Ref_len;
Ref_len= [0.135 0.287 0.434 0.25 0.274 0.141 0.353 0.434 0.36];
global Ref_minertia;
Ref_minertia= [0.001216 0.0148 0.1220 0.0990 0.2081 0.0020 0.0481 0.1360 0.3536];
number_of_segments = size(mass_ratio,2);
disp(number_of_segments);
global segment_mass;
segmnet_mass= zeros(1,number_of_segments);

% each segment mass computed throgh mass ratio

   for i= 1:number_of_segments
   segment_mass = Horse_mass * mass_ratio/100;
   end
disp(segment_mass);
% reading the data from excel sheets
 for i = 2:Number_sheets
    Read_data=xlsread(Excelsheet_name,i);
    % disp(Read_data);
    [data_rows,data_cols]=size(Read_data);
    [jointforce_Y, jointforce_Z,joint_force, Moment_Mp] =
compute_forcesmoments(Read_data,data_rows,number_of_segments);
    %plot(Moment_Mp);
 end

function [jointforce_Y, jointforce_Z,joint_force, Moment_Mp ] =
compute_forcesmoments(data,num_rows,num_of_segments)

%Reading  Ground Reaction Forces and segment accelerations and vector
%angles from excel spreadsheet
% Zeroing the allocated rows and columns for the output
jointforce_Y= zeros(num_rows,num_of_segments+2);
jointforce_Z= zeros(num_rows,num_of_segments+2);
Moment_Mp   = zeros(num_rows,num_of_segments);
Markerposition_X = zeros(num_rows,2*num_of_segments);
Markerposition_Y= zeros(num_rows,2*num_of_segments);
Markerposition_Z= zeros(num_rows,2*num_of_segments);
CoMposition_X = zeros(num_rows,num_of_segments);
CoMposition_Y = zeros(num_rows,num_of_segments);
CoMposition_Z = zeros(num_rows,num_of_segments);
```

```
CoMacc_X = zeros(num_rows, num_of_segments);
CoMacc_Y = zeros(num_rows, num_of_segments);
CoMacc_Z = zeros(num_rows, num_of_segments);
Vectorangle = zeros(num_rows,num_of_segments);
Ang_acc = zeros(num_rows,num_of_segments);
Perpend_dist_Z = zeros(num_rows, num_of_segments);
Perpend_dist_Y = zeros(num_rows, num_of_segments);
Perpend_prox_Z = zeros(num_rows, num_of_segments);
Perpend_prox_Y = zeros(num_rows, num_of_segments);
joint_force = zeros(num_rows, 1);
Moment_Inertia = zeros(1,num_of_segments);
len_segment = zeros(1,num_of_segments);
global segment_mass;
global Ref_mass;
global Ref_len;
global Ref_minertia;

% Read Ground reaction forces into the array
for i=1:num_rows
   jointforce_Y(i,1) = data(i,2);
   jointforce_Z(i,1) = data(i,3);
   jointforce_Y(i,7) = data(i,4);
   jointforce_Z(i,7) = data(i,5);

end
% Read marker postion into the array
for i = 1:num_rows
    temp1 = 6;
    temp2 = 71;
   for j= 1:2 * num_of_segments
      if(j<=10)
       Markerposition_X(i,j)= data(i,temp1);
       Markerposition_Y(i,j)=data(i,temp1+1);
       Markerposition_Z(i,j)= data(i,temp1+2);
       temp1= temp1+3;
      elseif(j>10)
       Markerposition_Z(i,j)= data(i,temp2);
       Markerposition_Y(i,j)=data(i,temp2-1);
       Markerposition_X(i,j)= data(i,temp2-2);
       temp2 = temp2-3;
      end

   end
end
%disp(Markerposition_X);
% CoM position,CoM Acceleration, Vector angle and Angular acceleration into
```

```
% the arrays
for i= 1:num_rows
    temp3 = 70;
    temp4 = 99;
    temp5 = 126;
   for j = 1: num_of_segments
      CoMposition_X(i,j)= data(i,temp3);
      CoMposition_Y(i,j)= data(i,temp3+1);
      CoMposition_Z(i,j)= data(i,temp3+2);
      CoMacc_X(i,j)= data(i,temp4);
      CoMacc_Y(i,j)= data(i,temp4+1);
      CoMacc_Z(i,j)= data(i,temp4+2);
      Vectorangle(i,j)= data(i, temp5);
      Ang_acc(i,j)= data(i,temp5+9);
      temp3 = temp3+3;
      temp4 = temp4+3;
      temp5 = temp5+1;
   end
end
g =9.8;
disp(segment_mass);
% joint forces of fore and hind limbs
for i= 1:num_rows

   for j=1:5
         if(j==1)

         jointforce_Y(i,j+1)= segment_mass(j)*CoMacc_Y(i,j)- jointforce_Y(i,j);
         jointforce_Z(i,j+1) = segment_mass(j)*CoMacc_Z(i,j)- jointforce_Z(i,j)+
segment_mass(j)* g ;
         else
         jointforce_Y(i,j+1)= segment_mass(j)*CoMacc_Y(i,j)+jointforce_Y(i,j);
         jointforce_Z(i,j+1) = segment_mass(j)*CoMacc_Z(i,j)+ jointforce_Z(i,j)+
segment_mass(j)* g ;
         end

   end
end
%disp(jointforce_Y);


% Joint force calulations of hind limb
for i= 1:num_rows
   for j = 6:9
        if(j==6)
```

```
        jointforce_Y(i,j+2)= segment_mass(j)*CoMacc_Y(i,j)- jointforce_Y(i,j+1);
        jointforce_Z(i,j+2) = segment_mass(j)*CoMacc_Z(i,j)- jointforce_Z(i,j+1)+
segment_mass(j)* g ;
      else
      jointforce_Y(i,j+2)= segment_mass(j)*CoMacc_Y(i,j)+jointforce_Y(i,j+1);
      jointforce_Z(i,j+2) = segment_mass(j)*CoMacc_Z(i,j)+ jointforce_Z(i,j+1)+
segment_mass(j)* g ;
      end

  end
end

%plot(jointforce_Z);
%disp(jointforce_Z);
% computing moment of inertia of each segment
     % computing length of each segment and Rp & Rd

for i = 1:2:2*num_of_segments
  sum_dist = 0;
  for j = 1:5
    dist = sqrt((Markerposition_X(j,i) - Markerposition_X(j,i+1))^2 + (Markerposition_Y(j,i) -
Markerposition_Y(j,i+1))^2 + (Markerposition_Z(j,i) - Markerposition_Z(j,i+1))^2);
     %disp(dist);
     sum_dist= sum_dist + dist;
  end
  len_segment((i+1)/2) = sum_dist/5000;

end

    % Moment of inertia
    for i = 1: num_of_segments
      Moment_Inertia(1,i) = Ref_minertia(i) * segment_mass(i) * len_segment(i)*
len_segment(i)/(Ref_mass(i) * Ref_len(i));
    end
    %disp(Moment_Inertia);
    % computing the perpendicular distance
for i = 1:2:2*num_of_segments
  for j = 1:num_rows
     Perpend_dist_Y(j,(i+1)/2) = abs(Markerposition_Y(j,i)- CoMposition_Y(j,(i+1)/2))/1000;
     Perpend_dist_Z(j,(i+1)/2) = abs(Markerposition_Z(j,i)- CoMposition_Z(j,(i+1)/2))/1000;
     Perpend_prox_Y(j,(i+1)/2) = abs(Markerposition_Y(j,i+1)-
CoMposition_Y(j,(i+1)/2))/1000;
     Perpend_prox_Z(j,(i+1)/2) = abs(Markerposition_Z(j,i+1)-
CoMposition_Z(j,(i+1)/2))/1000;
  end
```

```
end

% Joint moment calculations of fore and hind limbs
for i= 1:num_rows

   for j=1:9
         if (j==1 || j==6)
         Moment_Mp(i,j) = Moment_Inertia(1,j)* Ang_acc(i,j)- jointforce_Y(i,j) *
Perpend_dist_Z(i,j) - jointforce_Z(i,j)* Perpend_dist_Y(i,j) - jointforce_Z(i,j+1) *
Perpend_prox_Y(i,j) + jointforce_Y(i,j+1) * Perpend_prox_Z(i,j);
         else
         Moment_Mp(i,j) = Moment_Inertia(1,j)* Ang_acc(i,j)+jointforce_Y(i,j+1) *
Perpend_dist_Z(i,j) + jointforce_Z(i,j+1)* Perpend_dist_Y(i,j) + jointforce_Z(i,j+2) *
Perpend_prox_Y(i,j) + jointforce_Y(i,j+2) * Perpend_prox_Z(i,j)+Moment_Mp(i,j-1);
         end
   end
end
for i = 1:num_rows
   for j = 1:num_of_segments+2
      joint_force(i,j)= sqrt(jointforce_Y(i,j) * jointforce_Y(i,j) + jointforce_Z(i,j) *
jointforce_Z(i,j));
   end
end
plot(joint_force);
disp(joint_force);
%plot(jointforce_Y);
%plot(jointforce_Z);
%plot(Moment_Mp);
end
```

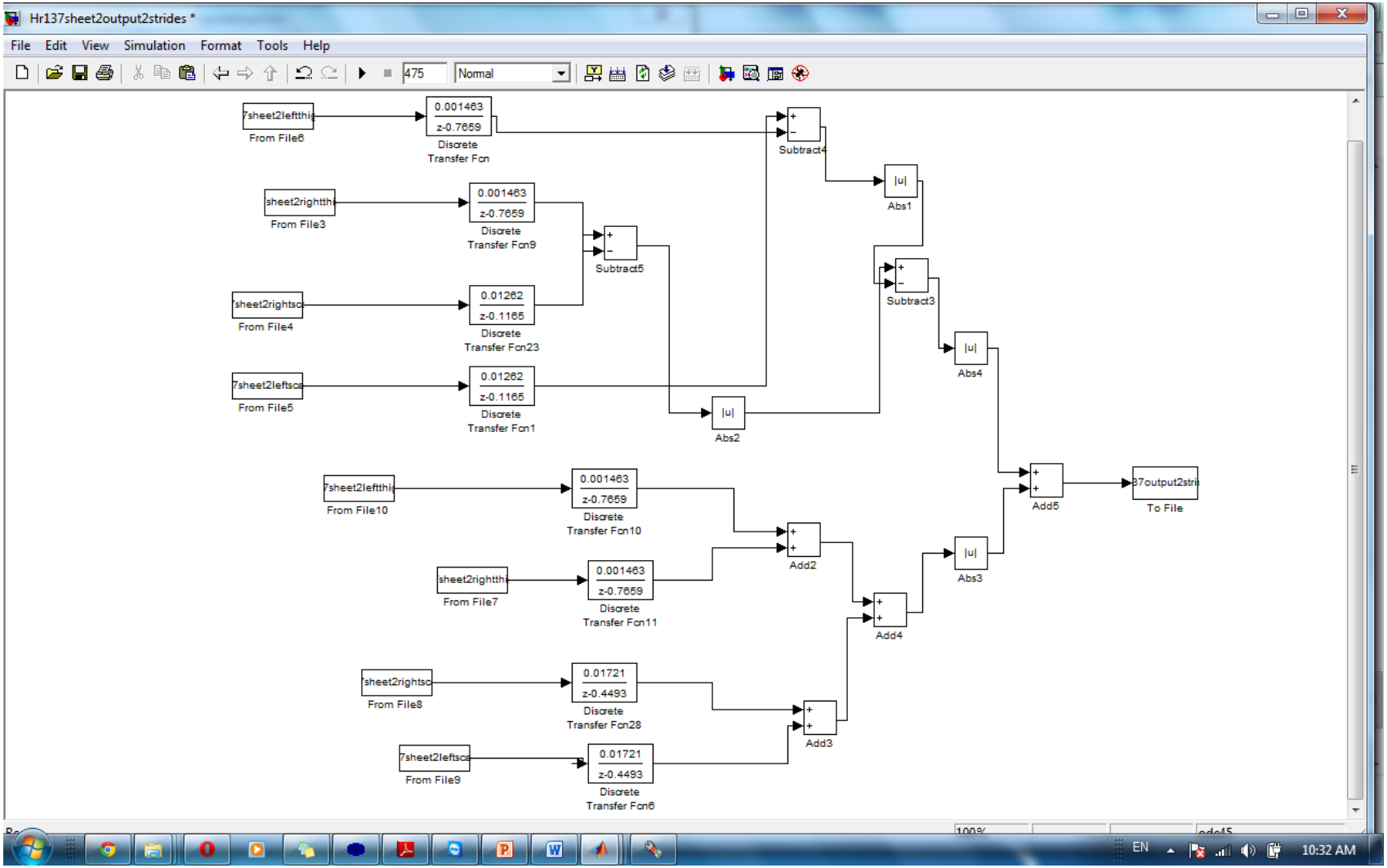

Simulink2010a model of the spring damper system to generate horse back forces with direct application of input to system transfer function

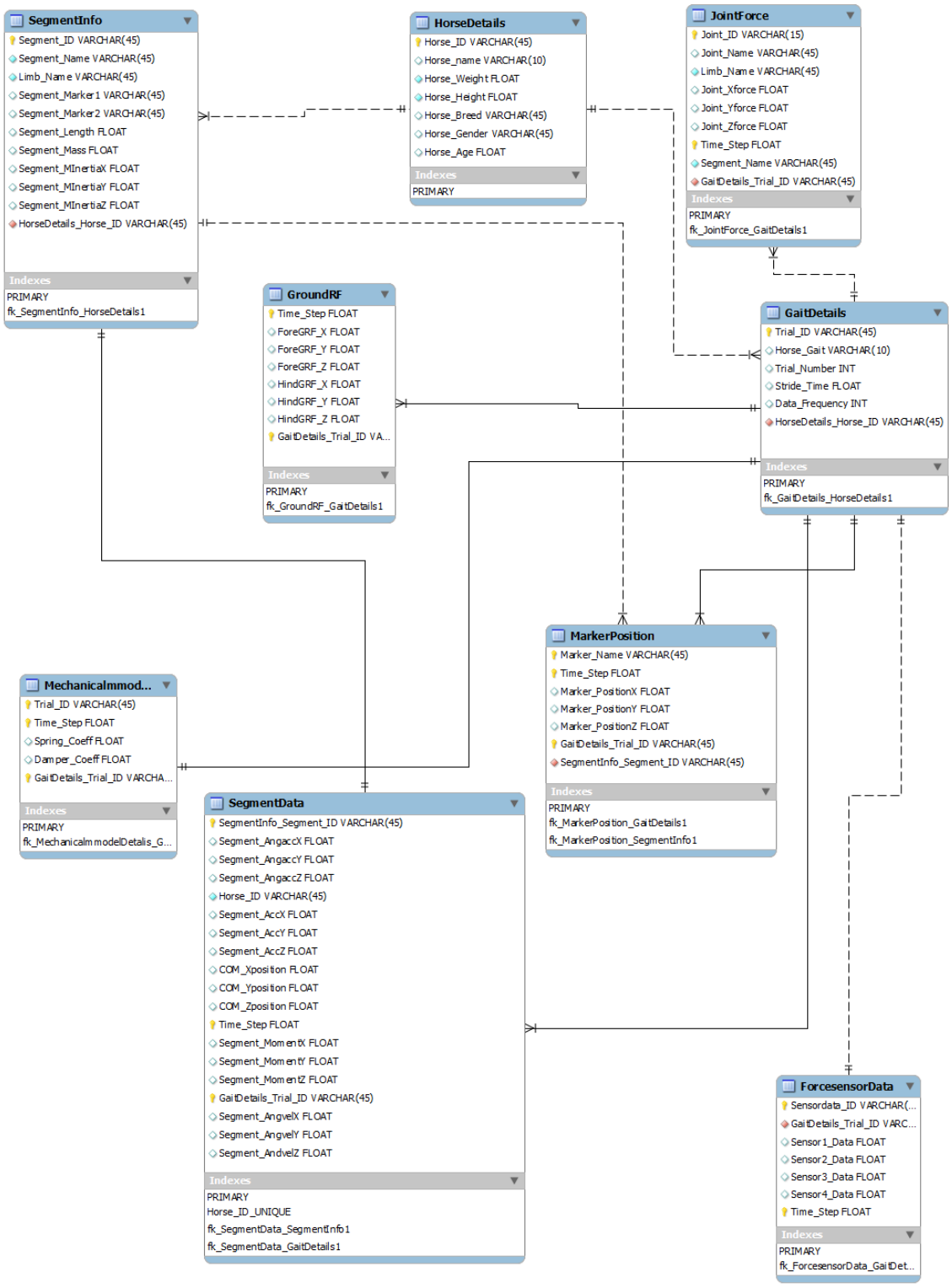

Entity- Relation diagram of the database for 3D inverse dynamic model

Vita

Laxmi Raghunandana Kaidapuram was born in March, 1986 in Nizamabad, Andhra Pradesh, India. She received her Bachelor of Technology in Electronics and Communication Engineering from Jawaharlal Nehru Technological University, Hyderabad, India, in the year 2007. After her graduation, she worked as a faculty member at Vignan Institute of Technological Sciences, Hyderabad, for one year. She then came to United States to pursue a Master of Science in Electrical Engineering degree at Louisiana State University (LSU). She worked as a graduate assistant from September 2008 to March 2011 in Laboratory of Equine and Comparative Orthopedic Research at School of Veterinary Medicine, LSU. She is expecting to graduate from electrical engineering in December of 2011.